Revisiting the Role of Hyperparasitism in the Evolution of Virulence

Simran K. Sandhu,[1] Andrew Yu. Morozov,[1,2,*] Robert D. Holt,[3] and Michael Barfield[3]

1. Department of Mathematics, University of Leicester, Leicester LE1 7RH, United Kingdom; 2. Institute of Ecology and Evolution, Russian Academy of Sciences, Moscow, Russia; and Lobachevsky State University of Nizhni Novgorod, Nizhniy Novgorod, Russia; 3. Department of Biology, University of Florida, Gainesville, Florida 32611

Submitted January 13, 2020; Accepted September 16, 2020; Electronically published December 23, 2020

Online enhancements: supplemental PDF.

ABSTRACT: Hyperparasitism denotes the natural phenomenon where a parasite infecting a host is in turn infected by its own parasite. Hyperparasites can shape the dynamics of host-parasite interactions and often have a deleterious impact on pathogens, an important class of parasites, causing a reduction in their virulence and transmission rate. Hyperparasitism thus could be an important tool of biological control. However, host-parasite-hyperparasite systems have so far been outside the mainstream of modeling studies, especially those dealing with eco-evolutionary aspects of species interactions. Here, we theoretically explore the evolution of life-history traits in a generic host-parasite-hyperparasite system, focusing on parasite virulence and the positive impact that hyperparasitism has on the host population. We also explore the coevolution of life-history traits of the parasite and hyperparasite, using adaptive dynamics and quantitative genetics frameworks to identify evolutionarily singular strategies. We find that in the presence of hyperparasites, the evolutionarily optimal pathogen virulence generally shifts toward more virulent strains. However, even in this case the use of hyperparasites in biocontrol could be justified, since overall host mortality decreases. An intriguing possible outcome of the evolution of the hyperparasite can be its evolutionary suicide.

Keywords: biological control, hyperparasite, coevolution, evolutionary suicide, pairwise invasibility plot (PIP), evolutionary attractor.

Introduction

Modeling evolution of host-parasite interactions is a rapidly growing area of theoretical research. An important group of parasites, which we focus on here (at times using the terms interchangeably) are pathogens, which by definition cause disease in their hosts. Recent theoretical studies emphasize the fact that evolution of pathogen virulence, disease transmission, and resistance can all be affected by other species in the ecological community, such as predators, and that these interactions can completely alter the evolutionary outcomes predicted using a classical host-parasite model (Morozov and Best 2012; Best 2018). An understudied dimension of the interplay of community dynamics and evolution is that host-parasite interactions often incorporate vertical chains, where a primary parasite is itself subject to parasitism by a secondary parasite, which is referred to as a hyperparasite (Beddington and Hammond 1977; Holt and Hochberg 1998; Parratt and Laine 2016). In many cases, hyperparasites are microbial pathogens, such as viruses (Milgroom and Cortesi 2004; Parratt and Laine 2016); however, macro-hyperparasites, such as insect hyperparasitoids, are also found in many systems and can play a fundamental role in shaping ecological communities (Holt and Hochberg 1998; Hassell 2000). The resultant chain becomes a host-parasite-hyperparasite system, which is somewhat similar to a tritrophic food web. However, dynamics of tritrophic nested parasite chains are often fundamentally different from those of predator-prey interactions (Holt and Hochberg 1998; Parratt and Laine 2016).

Hyperparasitism could potentially play a key role in the biological control of pests for two main reasons. Hyperparasites often debilitate their parasite hosts by reducing their deleterious impact on the basal host—thus facilitating recovery from the disease—and also hampering the transmission efficiency of the parasite. A hyperparasite can thus be a biological control agent that reduces the infection burden of the basal host (Dieckmann et al. 2005; Morozov et al. 2007; Parratt and Laine 2016). On the other hand, a hyperparasite can infect a parasite that itself is used as a control agent, thus undermining biocontrol efforts (May and Hassell 1981). In this case, the hyperparasite obviously acts as a nuisance in biocontrol. Finally, a hyperparasite that was initially introduced into the ecosystem as a biocontrol agent can, in the course of evolution, increase the ultimate virulence of the pathogen, thus producing a negative rather than a positive

* Corresponding author; email: am379@le.ac.uk.

Am. Nat. 2021. Vol. 197, pp. 216–235.
DOI: 10.1086/712351

effect on individual hosts (Taylor 2002). Understanding the long-term impact of hyperparasites on parasite and host dynamics and evolution is thus important for efficient virulence management and successful, evolutionarily stable biological control. Empirical examples of biological control via hyperparasites include attempts to control chestnut blight disease with viruses (Milgroom and Cortesi 2004), which is discussed further below; powdery mildew pathogens regulated by the fungus *Ampelomyces quisqualis* (Parratt et al. 2017); fungal hyperparasites controlling Dutch elm disease (Swinton and Gilligan 1999); and hyperparasites infecting fungi that in turn infect ants (Andersen et al. 2012) as well as bacteriophages infecting and killing human pathogens, such as *Vibrio cholerae* (Faruque et al. 2005).

Surprisingly, unlike two-component host-parasite models, tritrophic host-parasite-hyperparasite systems are still greatly understudied, especially the possible evolutionary outcomes in such systems (Taylor 2002; Parratt and Laine 2016). For example, we lack a coherent theoretical framework to analyze the evolution of virulence in host-parasite-hyperparasite systems, incorporating potential coevolutionary feedbacks. Such a framework should utilize recent developments in applying efficient mathematical and computational tools for modeling evolutionary dynamics, such as quantitative genetics (Abrams et al. 1993*a*; Day and Proulx 2004), adaptive dynamics (Geritz et al. 1997; Brännström et al. 2013), and, more generally, a game-theoretical approach in biology (Broom and Rychtár 2013). Our study is designed to partially bridge this existing gap in understanding and to provide a more quantitative description of the evolution of virulence in systems with hyperparasitism.

In this article, we focus on the potential shift in the evolutionary optimal virulence of a parasite caused by the introduction of a hyperparasite, along with shifts in host dynamics. Here, the virulence of a parasite describes how harmful it is to its host, which we assume positively correlates with parasite transmission rate; this idea of a relationship between the parasite virulence and transmission rate is termed the trade-off hypothesis (Anderson and May 1982; Alizon et al. 2009). We extend a generic host-parasite-hyperparasite model previously introduced by Holt and Hochberg (1998) and explored in more detail by Taylor (2002) and Taylor et al. (1998) by explicitly considering the dynamics of numbers of hosts infected by various strains of the parasite and/or hyperparasite and including the effects of density dependence. Using this model, we first explore the evolution of parasite virulence for the scenario where only one species (i.e., either the parasite or the hyperparasite) evolves, with the life-history traits of the other species being fixed. Then we consider the case of coevolution of the parasite and the hyperparasite.

We find that introduction of a hyperparasite into the original host-parasite system generally shifts the evolutionarily optimal virulence of the pathogen (that attained in the absence of the hyperparasite) toward higher virulence. However, this does not necessarily signify a failure of biological control, since in the presence of the hyperparasite the model also predicts an increase in the number of healthy hosts and a decrease in the overall mortality load. Finally, we show some intriguing results, such as the finding that the presence of evolutionary bistability and long-term coevolution of the hyperparasite in the system can result in coevolutionary extinction of the hyperparasite.

Model Equations and General Framework

Our host-parasite-hyperparasite model involves three main host population compartments: uninfected susceptible hosts (S), parasitized hosts (P), and hyperparasitized hosts (H), with the total number of hosts equal to N. Hyperparasitized hosts, of course, have both a parasite and a hyperparasite, but to simplify the terminology, "parasitized hosts" refers only to those with a parasite and no hyperparasite. The inspiration for this model was a particular system of biological control of chestnut blight disease (Milgroom and Cortesi 2004). In our model, the healthy hosts S would represent uninfected healthy chestnut trees, the parasitized hosts P would be trees infected by the disease-causing fungus *Cryphonectria parasitica*, and the hyperparasitized hosts H would represent the trees infected by the hypovirus introduced as a biological control agent. Although this was the inspiration for our model, it is not the only applicable example, as considered in greater detail in "Discussion."

Within the compartments P and H we consider different parasite and hyperparasite strains denoted, respectively, by subscripts i and L. In other words, P_i signifies the number of parasitized hosts containing parasite strain i, and $H_{i,L}$ is the number of hyperparasitized hosts infected by a parasite of strain i that is in turn hyperparasitized by strain L. We assume that all hosts are born uninfected at a rate dictated by a density-dependent function $F(N)$, with only susceptible hosts being able to reproduce. Parasites are transmitted when a susceptible host comes into contact with a parasitized host (this does not have to be physical contact, as long as transmission by whatever means is proportional to the product of densities of susceptible and parasitized hosts). Transmission of the hyperparasite can occur either via susceptible hosts or parasitized hosts coming into contact with a hyperparasitized host. It is assumed that the transmission of parasites and hyperparasites are coupled, meaning that a hyperparasite cannot be successfully transmitted without its parasite when they initially infect a new host. When transmission occurs to a parasitized host P_i from a hyperparasitized host $H_{j,L}$, either the introduced parasite j is excluded (i.e., the hyperparasite spreads among the resident

parasite strain, which excludes the invading parasite) or the resident parasite i is replaced (i.e., the invading parasite displaces the resident parasite). The probability of this invading parasite being excluded is described by the parameter Q. Note that we assume the hyperparasite is always physically dispersed within propagules of the parasite.

The system is an extension of previous models analyzed in Taylor et al. (1998), Taylor (2002), and Morozov et al. (2007), which ecologically incorporate a form of intraguild predation. Here, we explicitly consider the dynamics of multiple competing strains of parasite and hyperparasite because we are interested in their evolution, going beyond their purely ecological dynamics. Section SM3 in the supplemental PDF (available online) analyses the one-strain version of these equations; there it is shown that the system with single strains of both the parasite and the hyperparasite can achieve an equilibrium and that this equilibrium is locally stable, provided it exists. Here, we also assume for simplicity that once a host has been infected it is impossible for it to recover back to its susceptible state.

The model equations for S, P_i, and $H_{i,L}$ with n parasite and m hyperparasite strains are as follows:

$$\frac{dS}{dt} = F(N)S - \mu S - S\sum_{i=1}^{n}\left(\beta_P(\alpha_i)P_i + \sum_{K=1}^{m}\beta_H(\alpha_i,\epsilon_K)H_{i,K}\right), \tag{1}$$

$$\frac{dP_i}{dt} = \beta_P(\alpha_i)SP_i - P_i\sum_{j=1}^{n}\sum_{K=1}^{m}\sigma(\alpha_j,\epsilon_K)H_{j,K} - \mu P_i - \alpha_i P_i, \tag{2}$$

$$\begin{aligned}\frac{dH_{i,L}}{dt} = {} & \beta_H(\alpha_i,\epsilon_L)SH_{i,L} + QP_i\sum_{j=1}^{n}\sigma(\alpha_j,\epsilon_L)H_{j,L} \\ & + (1-Q)\sigma(\alpha_i,\epsilon_L)H_{i,L}\sum_{j=1}^{n}P_j - \mu H_{i,L} \\ & - \alpha_H(\alpha_i,\epsilon_L)H_{i,L}.\end{aligned} \tag{3}$$

Note that there is an equation (2) for each parasite strain and an equation (3) for each parasite-hyperparasite strain combination. The parasite strain is described by the parasite virulence α, whereas the hyperparasite strain is governed by both the corresponding parasite virulence α and the hyperparasite strength ϵ. This hyperparasite strength is the debilitating impact of the hyperparasite on the parasite. For example, this can be a decrease in metabolic rates or in division rate. The terms $\beta_P(\alpha_i)SP_i$ and $\alpha_i P_i$ describe, respectively, the transmission rate and the infection-related mortality of P_i. The terms $\beta_H(\alpha_i,\epsilon_L)SH_{i,L}$ and $\sigma(\alpha_i,\epsilon_L)P_iH_{i,L}$ are transmission rates from hyperparasitized hosts of type $H_{i,L}$ to the two possible hosts S and P_i, respectively; $\alpha_H(\alpha_i,\epsilon_L)H_{i,L}$ is the mortality of these hyperparasitized hosts. The parameter Q denotes the probability that when a parasite of type i with hyperparasite L infects a host parasitized by parasite j, a hyperparasitized host of type $H_{j,L}$ is produced (thus, the hyperparasite invades the resident parasite and the invading parasite strain is excluded by the resident parasite strain); otherwise, with probability $1-Q$ the resultant hyperparasitized host will be $H_{i,L}$ (the invading parasite and its hyperparasite jointly displaces the resident parasite). As in Taylor et al. (1998), Taylor (2002), and Morozov et al. (2007), we do not consider coinfections, which we acknowledge may change model predictions (Alizon and van Baalen 2008). This means that a different parasite cannot infect a parasitized host and displace the resident parasite unless the invading parasite carries a hyperparasite (and we used Q near 1, so this was unlikely, and Q in any case did not affect a parasite's invasibility). Finally, μ is the parasite-independent (and density-independent) mortality rate of hosts. The meaning of the parameters is briefly summarized in table 1 and a detailed flowchart of the model is provided in section SM1 of the supplemental PDF.

The key novel feature of the current framework is that we can separately model evolution of the parasite and the hyperparasite (assuming the other species is fixed) as well as their coevolution. In earlier models, infection of a parasitized host (P_j) by a parasite-hyperparasite pair ($H_{i,L}$) was assumed to always result in the exclusion of the original parasite strain; that is, parasite strain j was excluded and replaced by parasite strain i and hyperparasite strain L. Although such a displacement is possible in principle, it is also logical to assume that if a host is heavily parasitized by parasite strain j, then strain j may not be replaced by strain i and instead the host becomes hyperparasitized with parasite strain j and hyperparasite strain L. In our model, we quantify this idea by assuming Q to be close to 1 in most cases (the assumption in earlier models corresponds to $Q = 0$). Mathematically, we can consider equations (1)–(3) for any number of strains and any parameters describing parasite and hyperparasite life-history traits. Biologically, however, effects of genetic incompatibility of hyperparasites can play a role; that is, a hyperparasite living on a certain parasite strain may not be able to infect a parasite strain with a different genetic background (Taylor 2002; Milgroom and Cortesi 2004). In this article, we will neglect the effects of such incompatibility by considering that all combinations of parasite and hyperparasite strains occur as a result of small mutations that do not create genetic barriers for hyperparasite transmission.

The main goal of the current study is to explore the evolution and coevolution of parasite virulence (α) and hyperparasite strength (ϵ) in a host-parasite-hyperparasite system. To achieve this goal, we first investigate the evolution of the parasite in the presence of a hyperparasite when

Table 1: Definitions of variables, parameters, and functions used in the host-parasite-hyperparasite model defined by equations (1)–(3)

Model component	Meaning
S	Density of uninfected (susceptible) hosts
P_i	Density of parasitized hosts infected by uninfected parasites of strain i
$H_{i,L}$	Density of hyperparasitized hosts infected by parasites of strain i infected by hyperparasites of strain L
$F(N)$	Density-dependent birth rate of susceptible hosts (N is total host density)
μ	Natural host density-independent mortality due to factors other than infection, under the assumption that $0 \le \mu \le 1$
α_i	Virulence of uninfected parasites of strain i, with $0 \le \alpha_i$
ϵ_L	Hyperparasite strength of strain L
$\alpha_H(\alpha_i, \epsilon_L)$	Virulence of parasites of strain i infected by hyperparasites of strain L; defined as $\alpha_H(\alpha_i, \epsilon_L) = \alpha_0(\epsilon_L)\alpha_i$, with $0 \le \alpha_0(\epsilon_L) \le 1$ for hypovirulence and $\alpha_0(\epsilon_L) \ge 1$ for hypervirulence
$\beta_P(\alpha_i)$	Transmission rate from parasitized hosts P_i to susceptible hosts S
$\beta_H(\alpha_i, \epsilon_L)$	Transmission rate from hyperparasitized hosts $H_{i,L}$ to susceptible hosts S; defined as $\beta_H(\alpha_i, \epsilon_L) = \beta_0(\epsilon_L)\beta_P(\alpha_i)$
$\sigma(\alpha_i, \epsilon_L)$	Transmission rate from hyperparasitized hosts $H_{i,L}$ to hosts parasitized by any strain, which is defined as $\sigma(\alpha_i, \epsilon_L) = \sigma_0\beta_H(\alpha_i, \epsilon_L)$
Q	When an infected parasite invades a parasitized host, the probability that its hyperparasite spreads throughout the resident parasite (which is not displaced by the invasive parasite strain); $1 - Q$ is the probability that the invading parasite (with its hyperparasite) displaces the resident

the life-history traits of the latter are fixed. Then we fix the life-history traits of the parasite and consider the evolution of the hyperparasite alone. Finally, we model the coevolution of the parasite and hyperparasite together. In each of these cases, it is assumed that the trait values for all strains are parameterized by α and ϵ. To reduce the complexity of model (1)–(3), it is then assumed that initially each species is a monomorphic population with traits α_r and ϵ_r, whose ecological dynamics are governed by equations (1)–(3) with a single strain of parasite and hyperparasite (the equations become [D1]–[D3], with $\alpha = \alpha_r$ and $\epsilon = \epsilon_r$). It is further assumed that mutant strains arise in the evolving populations and the trait values of those mutants (α_m, ϵ_m) are (infinitesimally) small perturbations away from the resident trait values. This then allows one to use the adaptive dynamics framework (which assumes continuous trait values) to determine how the trait values for the evolving populations continuously change over time.

Following a well-established approach, we assume a trade-off between the virulence and transmission rate of a parasite and between the virulence and transmission rate of a hyperparasite-infected parasite relative to an uninfected parasite (Lipsitch and Moxon 1997; Ebert and Bull 2003; Alizon et al. 2009). Note that such trade-offs are expressed by a positive relationship between transmission (high values are good for the parasite) and virulence (high values are bad for the parasite); such trade-offs have been demonstrated empirically (Alizon et al. 2009; Doumayrou et al. 2013). In the absence of the hyperparasite, we model the parasite trade-off by making β_P a function of α, as is often assumed (Alizon et al. 2009). Infection with a hyperparasite usually decreases both the virulence and the transmission of the parasite, but to different degrees (Milgroom and Cortesi 2004).

To incorporate the dependence of the hyperparasite's detriment to parasites on the hyperparasite strength ϵ, we use the following generic structure of the functions in the presence of the hyperparasite: $\alpha_H(\alpha, \epsilon) = \alpha_0(\epsilon)\alpha$, $\beta_H(\alpha, \epsilon) = \beta_0(\epsilon)\beta_P(\alpha)$, and $\sigma(\alpha, \epsilon) = \sigma_0\beta_H(\alpha, \epsilon)$, where σ_0 is the transmission of a hyperparasite-infected parasite to a parasitized host relative to its transmission to a susceptible host. These formulations allow the introduction of trade-offs into the model; we investigate various mathematical formulations for $\beta_P(\alpha)$, $\alpha_0(\epsilon)$, and $\beta_0(\epsilon)$ (see the next section for details). The presence of the hyperparasite is characterized by its strength ϵ, which determines its impact on parasite virulence through the function $\alpha_0(\epsilon)$ (the virulence of the parasite with the hyperparasite relative to uninfected parasite virulence) and its transmission through the relative transmission function $\beta_0(\epsilon)$. In examining coevolution, we consider the virulence of the pathogen α and the strength of the hyperparasite ϵ to be independent evolutionary parameters.

In most examples in this article, we assume that $0 \le \alpha_0(\epsilon) \le 1$ (known as hypovirulence): a value approaching zero signifies a very large decrease in parasite virulence with hyperparasite infection, whereas $\alpha_0(\epsilon) = 1$ means no impact. In some cases, however, the hyperparasite may induce hypervirulence (e.g., a virus infecting the human infectious agent *Staphylococcus aureus* produces an enzyme that permits the microbe to be "below the radar" of the human immune system; Gerlach et al. 2018), where $\alpha_0(\epsilon) > 1$, meaning that the hyperparasitized parasite is

more detrimental to its host (Brüssow et al. 2004; Parratt and Laine 2016). We will briefly consider this case.

Computationally, we apply two powerful approaches to modeling evolution. The first one applies the adaptive dynamics framework (Geritz et al. 1997; Brännström et al. 2013), a versatile tool with applications in a wide range of diverse areas, including epidemiology (Dieckmann et al. 2005; Boldin and Diekmann 2008; Svennungsen and Kisdi 2009). A key feature of adaptive dynamics is the link between population and evolutionary dynamics, thereby incorporating and generalizing the fundamental idea of frequency-dependent selection from game theory. This modeling approach considers the long-term evolutionary outcomes of an invasion of a rare mutant parasite or hyperparasite into the environment formed by a resident at ecological equilibrium (or any other type of attractor). The outcome can be characterized by the invasion fitness (inferred from the initial growth rate of the rare invading mutant), which when positive indicates a successful invasion; subsequently, the mutant displaces the resident. This process occurs iteratively, with successive invasions of mutants that, when successful, exclude the resident type (Eshel 1983; Taylor 1989; Christiansen 1991; Abrams et al. 1993*b*). Following a large number of such invasions and substitutions, the species will evolve toward an evolutionarily singular point, at which the selection gradient (defined as the derivative of the invasion fitness) vanishes. To locate all singularities we apply both analytical methods and direct numerical simulations in which we randomly introduce mutants and solve the corresponding differential equations for the dynamics of mutants and residents to verify the outcome of an invasion.

Subsequent evolutionary behavior depends on the stability of the evolutionary singularity (Taylor 1989; Abrams et al. 1993*b*), which can be determined from a pairwise invasibility plot (PIP; Kisdi and Meszéna 1993) and/or by computing the second derivatives of the invasion fitness at a singular point (Eshel 1983; Geritz et al. 1998). PIPs are graphical illustrations of the invasion success of potential mutants, often used to study the consequence of invasions and substitutions. These plots show, for each resident trait, all of the mutant traits for which the invasion fitness is positive and therefore results in a successful invasion. The singularities can be stable (an evolutionary attractor), unstable (an evolutionary repeller), or a branching point. An evolutionary attractor occurs when a singular point is both an evolutionarily stable strategy (ESS)—nearby mutants are not able to invade—and a convergent stable strategy. These joint conditions ensure that an ESS can be attained and maintained (Eshel 1983). If the singularity is convergent stable but not an ESS, then we have a branching point, where an initially monomorphic population becomes dimorphic (for examples, see Dieckmann and Doebeli 1999; Doebeli 2011). However, for our model we have shown that branching behavior is impossible, implying that a singularity will be either an evolutionary attractor or a repeller (see app. C).

The second computational approach uses a quantitative genetics framework where we model the evolution of life-history traits directly, following Abrams et al. (1993*a*) and Day and Proulx (2004). The equations for the species densities and life-history traits are modified from the model described above. The first three equations of the model describe the mean field variation of S, P, and H (all model parameters have the same meaning as above). Two equations are added describing the evolution of the parasite and hyperparasite traits α and ϵ, which govern transmission. For the full equations, see appendix D.

Results

Evolution in the Parasite Alone

Consider the scenario where the hyperparasite does not evolve (i.e., ϵ is fixed) but there is evolution of parasite virulence, α. We assume that the parasite transmission $\beta_P(\alpha)$ is monotonically increasing with parasite virulence α and passes through the origin. Thus, there is no parasite transmission without an increase in host mortality.

To find ESSs in the system using adaptive dynamics, we consider the dynamics of a rare mutant introduced into a resident population (i will be set to m for the mutant and r for the resident). The dynamics of hosts with the mutant parasite without (P_m) and with (H_m) the hyperparasite (as long as the latter are rare) are given by (for simplicity we omit the second index in H)

$$\frac{dP_m}{dt} = \beta_P(\alpha_m)S^*P_m - \sigma(\alpha_r)P_mH_r^* - \mu P_m - \alpha_m P_m, \quad (4)$$

$$\begin{aligned}\frac{dH_m}{dt} = {} & \beta_H(\alpha_m)S^*H_m + Q\sigma(\alpha_r)P_mH_r^* \\ & + (1-Q)\sigma(\alpha_m)P_r^*H_m - \mu H_m - \alpha_H(\alpha_m)H_m,\end{aligned} \quad (5)$$

where S^*, P_r^*, and H_r^* are the stationary states of the resident population (determined by eqq. (1)–(3) with one strain each of parasite and hyperparasite; see sec. SM3 of the supplemental PDF) and α_m and α_r are, respectively, the virulence of the mutant and resident strains. The flowchart for this model is shown in figure S2 (figs. S1–S19 are available online).

The invasion fitness of the mutant parasite is given by the largest eigenvalue of the Jacobian matrix of model (4) and (5). In appendix A, we derive the invasion fitness (following the assumptions of adaptive dynamics that mutations will occur in very small steps, meaning that α_m

is close to α_r) and the related evolutionarily singular point(s). For small mutations, invasion fitness is

$$\lambda_P = \beta_P(\alpha_m)S^* - \sigma(\alpha_r)H_r^* - \mu - \alpha_m. \quad (6)$$

By computing the corresponding derivatives (Eshel 1983), we analytically found that for a concave trade-off function $\beta_P(\alpha)$, any evolutionarily singular point is always evolutionary and convergence stable (i.e., it is an evolutionary attractor): thus, long-term evolution will eventually reach this point. This can be illustrated by plotting a PIP for the virulence of the parasite (α), as shown in figure 1*A* constructed for a hyperbolic $\beta_P(\alpha)$. This diagram shows the sign of the invasion fitness (a positive sign implies that the mutant can invade). A singular point is located at the intersection of a boundary between positive and negative invasion fitness and the principal diagonal. This describes the ultimate evolutionary state of the system.

We investigated the dependence of the ESS virulence (α^*) on key model parameters. Figure 1*B* and figure 1*C* show how altering the background mortality μ would affect the ESS virulence of the parasite and the stationary densities of the host. We choose to investigate the dependence on the background mortality μ of the host, as it can be affected by plenty of ecological and environmental factors (such as predators, climate, and human intervention, like harvesting). For the range of parameters that we considered, we verified the stability of the host equilibria in all three regions of figure 1*B* using standard analytical techniques (for details, see sec. SM3 of the supplemental PDF).

From figure 1*B* and figure 1*C* we can see that at low mortality μ the parasitized hosts cannot coexist with the hyperparasitized hosts (i.e., lower virulence is favored when background mortality is low). In this case, all hosts infected by the parasite are also infected by the hyperparasite. Under the considered scenario and at low values of μ, we have a competition between different strains of parasites (more virulent and less virulent) containing the same strain of hyperparasite. Coexistence of both the parasitized host and the hyperparasitized host, P and H, is possible only for some intermediate μ. At high rates of μ, the hyperparasite cannot survive and becomes extinct (higher transmission is favored when natural mortality is high). This extinction of hyperparasites at high values of μ can be explained by the fact that the parasite without the hyperparasite has an advantage, since its transmission is higher (compared with that of the parasite containing the hyperparasite). On the contrary, the mortality of infected hosts (at high values of μ) is mostly affected by background mortality rather than the virulence. In the absence of the hyperparasite, the parasite virulence α evolves to intermediate values, which therefore leads to intermediate host mortality rates. Interestingly, in the presence of the hyperparasite, the parasite virulence α evolves to higher values (compared with the hyperparasite-free scenario), which leads to higher mortality rates for parasitized hosts. However, as hyperparasites reduce the host

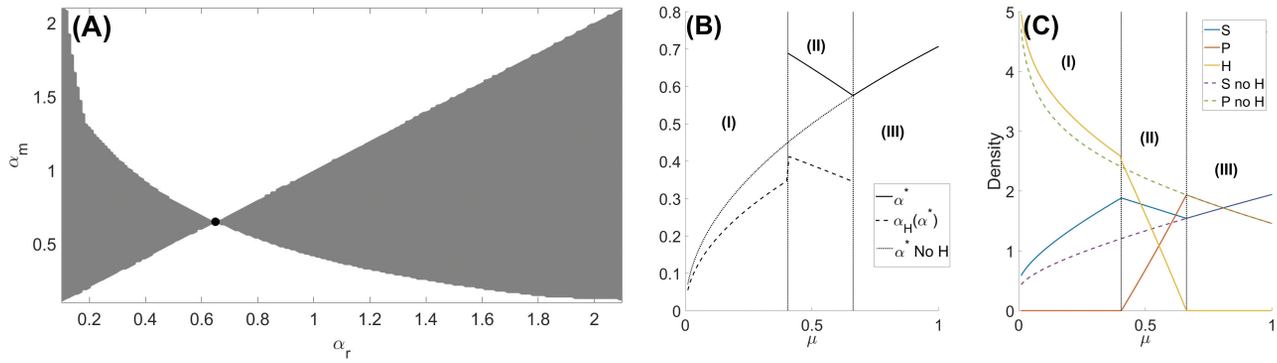

Figure 1: *A*, Pairwise invasibility plot describing the long-term evolution in model (1)–(3) in the case of evolution of parasite virulence α only. The gray regions represent positive invasion fitness, and the white regions represent the domain where invasion fitness is negative. For the whole plane, the invasion fitness was defined as $\max(\lambda_H, \lambda_P)$ and computed numerically. The evolutionarily singular strategy is an evolutionary attractor shown by a black circle for $\mu = 0.5$. *B*, Dependence of evolutionarily stable strategy (ESS) virulence on background mortality μ. The graph shows the ESS virulence α^* (solid black curve), the corresponding virulence of the hyperparasitized host (dashed black curve), and the ESS virulence that would evolve if the system had no hyperparasite (dotted black curve). *C*, Stationary host densities as functions of μ. The blue curve represents the stationary density of susceptible hosts, the orange curve represents the stationary density of parasitized hosts, and the yellow curve represents the stationary density of the hyperparasitized host. The dashed purple and green lines represent the susceptible and parasitized host densities, respectively, in the absence of the hyperparasite. Regions of the graph are as follows: I = at the equilibrium, all parasites are infected by the hyperparasite; II = coexistence of uninfected hosts and infected hosts with and without the hyperparasite; III = the hyperparasite cannot be established in the system, with the resulting system consisting of just susceptible hosts and hosts infected by the parasite. All other parameter values are as follows: $F(N) = 5 - 0.8N$, $Q = 0.9$, $\beta_0 = 0.5$, $\sigma_0 = 0.5$, $\alpha_0 = 0.6$, and $\beta_P = \alpha C/(\alpha + K)$, with $C = 1.5$ and $K = 0.5$.

mortality, the actual mortality rates averaged over all infected hosts is lower than what would be experienced in the absence of hyperparasites.

This result can also be observed from the graphs of the prevalence and mortality rates; for example, the overall mortality of hosts is still lower in the presence of the hyperparasite (see sec. SM2 of the supplemental PDF). Note that here we are mostly interested in the overall host mortality (rather than the mortality of only infected hosts), since the purpose of introducing the hyperparasite as a biological control agent is to reduce the average overall mortality. We observed an increase in the density of susceptible hosts S after the addition of the hyperparasite, as the overall infection rate $\beta_P(\alpha)P + \beta_H(\alpha, \epsilon)H$ is reduced as a result of reduced transmission with the hyperparasite. Average mortality is, therefore, reduced not only because hyperparasitized hosts have lower virulence than parasitized hosts but also because there are more susceptible hosts with the lowest mortality. Therefore, average mortality is reduced even with the evolution of higher virulence in parasitized hosts (this result holds for all mortality rates $0.05 \leq \mu \leq 1$; for very low rates [i.e., $\mu < 0.05$] we observe that the overall mortality is slightly higher in the presence of the hyperparasite than in the absence of the hyperparasite). We have also investigated the influence of parameters α_0 (which is the reduction of virulence of the parasite in the presence of the hyperparasite) and β_0 (which is the reduction of the transmission of the parasite in the presence of the hyperparasite) and found a dependence similar to that for μ (supplemental PDF, sec. SM2).

Importantly, the observed increase in the ESS virulence of the parasite in the presence of the hyperparasite is not constrained to our particular choice of the trade-off function $\beta_P(\alpha)$. This property is more generic, as formulated in the theorem below.

> THEOREM 1. If the trade-off between virulence and transmission rate is such that β_P is given by some increasing function with a negative second derivative and mutations occur in small steps, then $\alpha^* \geq \hat{\alpha}$, where α^* is the ESS in the presence of both the parasite and the hyperparasite and $\hat{\alpha}$ is the ESS in the absence of the hyperparasite.

The proof of theorem 1 is given in appendix B. This shows quite generally that introducing a hyperparasite is expected to increase the evolutionarily stable virulence of the parasite. Furthermore, we can also show that the stationary densities of susceptible hosts increase after the introduction of the hyperparasite despite this increase in virulence, clearly demonstrating the positive impact the hyperparasite can have, for instance, in biological control efforts (full details are shown in app. B).

We should note that the ESS values of virulence do not depend on the parameter Q quantifying the probability of displacement of the pathogen strain as a result of infection by another parasite strain containing a hyperparasite. Mathematically, this somewhat counterintuitive observation can be explained by the fact that the expressions for the invasion fitness and the resident strain stationary densities do not actually include Q. The resident densities do not include Q because they have only one strain of parasite, so there is no displacement possible. The invasion fitness does not include Q because the Jacobian has a zero at upper right, so the eigenvalues are the diagonal elements and the largest is the one due to the parasite equation, which does not include Q. The same holds true for the other evolutionary scenarios considered below.

Evolution in the Hyperparasite Only

Now we consider the opposite scenario, where the life-history traits of the parasite are fixed and only the hyperparasite evolves. The evolving parameter is the hyperparasite strength ϵ. The impact of the hyperparasite on the transmission rate β_H (which also affects σ) is described by multiplication of the uninfected parasite rate by the factor $\beta_0(\epsilon)$; the effect of the hyperparasite on the parasite virulence α is given by multiplication by $\alpha_0(\epsilon)$. We generally assume that $\alpha_0(\epsilon)$ and $\beta_0(\epsilon)$ are positive increasing functions (as the greater the hyperparasite strength ϵ, the greater the hyperparasite virulence and transmission) and consider several possible mathematical formulations (fig. 2). Generally, we assume $0 \leq \alpha_0(\epsilon) \leq 1$ and $0 \leq \beta_0(\epsilon) \leq 1$ (thus, the hyperparasite reduces parasite virulence and transmission).

The equation for a rare mutant hyperparasite H_m invading a resident strain of the hyperparasite at the ecological equilibrium (S^*, P_r^*, H_r^*) is

$$\frac{dH_m}{dt} = (\beta_H(\epsilon_m)S^* + \sigma(\epsilon_m)P_r^* - \mu - \alpha_H(\epsilon_m))H_m = \lambda_H(\epsilon_m)H_m, \tag{7}$$

where $\lambda_H(\epsilon_m)$ is the invasion fitness. The corresponding flowchart of the model is provided in the supplemental PDF.

By applying the adaptive dynamics framework we explored evolutionarily singular points in the model. In particular, for this model it is straightforward to prove that a singular point is either an evolutionary attractor (this implies convergence stability) or a repeller (we do not show here the mathematical derivations for brevity). The evolutionary outcome depends on the shape of α_0 and β_0. In this study, we considered various combinations

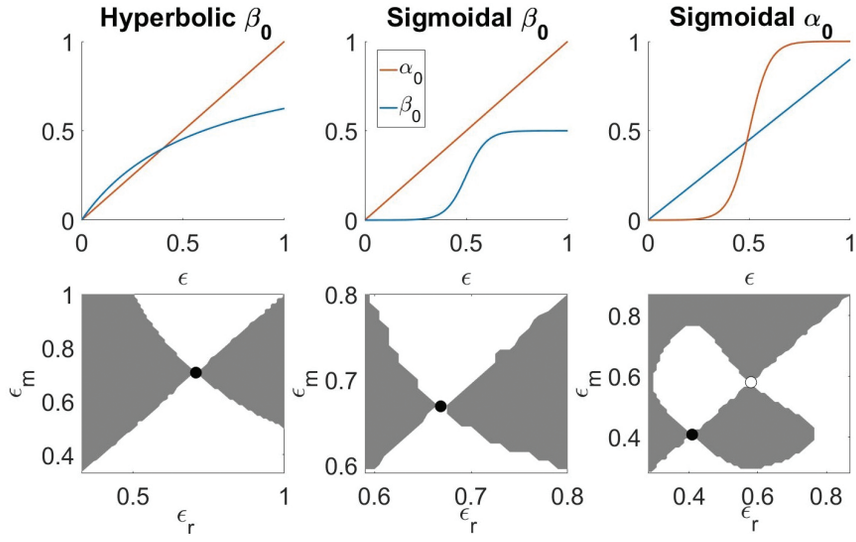

Figure 2: The top panels show the various trade-off functions for α_0 and β_0 corresponding to the pairwise invasibility plots describing the long-term evolution in the system. The bottom panels show the invasion fitness plotted in the plane (ϵ_r, ϵ_m) using (7). The gray regions represent positive λ_H (and therefore invasion fitness), and the white regions represent the domain where the invasion fitness is negative. The evolutionarily singular strategy is an evolutionary attractor shown by a black circle. Starting from the left panels, the trade-off functions are given by $\alpha_0(\epsilon) = \epsilon$, with hyperbolic $\beta_0(\epsilon) = \epsilon/(0.6 + \epsilon)$; $\alpha_0(\epsilon) = \epsilon$, with sigmoidal $\beta_0(\epsilon) = 0.5/(1 + \exp(-20(\epsilon - 0.5)))$; and sigmoidal $\alpha_0(\epsilon) = 1/(1 + \exp(-20(\epsilon - 0.5)))$, with $\beta_0(\epsilon) = 0.9\epsilon$. All other parameter values are as follows: $F(N) = 5 - 0.8N$, $\mu = 0.5$, $Q = 0.9$, $\sigma_0 = 0.5$, $\alpha = 0.6$, and $\beta_P = \alpha C/(\alpha + K)$, with $C = 1.5$ and $K = 0.5$.

of the trade-off functions, three of which are shown in figure 2. The top panels present the functional forms $\alpha_0(\epsilon)$ and $\beta_0(\epsilon)$, and the bottom panels show the corresponding PIPs. One can see from the figure (*right panels*) that in the case of a sigmoidal $\alpha_0(\epsilon)$ and a linear $\beta_0(\epsilon)$ the evolutionary outcome depends on the starting point. If we start from an ϵ to the right of the repeller (shown by the open circle), then the hyperparasite strength will evolve toward the maximum value of ϵ. Note that such bistability can occur only under the assumption that the life-history traits of mutants are small perturbations of that of the resident: if mutations of any size could occur, then the maximum value of ϵ will always be the evolutionary end point. We also considered the scenario with a linear $\beta_0(\epsilon)$ and a hyperbolic $\alpha_0(\epsilon)$ as well as the case where $\alpha_0(\epsilon)$ is hyperbolic but $\beta_0(\epsilon)$ is linear; however, we found that in both cases an ESS is impossible. Note that for the case of a sigmoidal $\alpha_0(\epsilon)$ resulting in two evolutionarily singular strategies, we show the corresponding ESS point.

As in the previous section, we investigated the dependence of the ESS of the hyperparasite on key model parameters, in particular, on the variation of mortality μ, as shown in figure 3. We observe from figure 3 that again at low background mortality, all of the parasites carry the hyperparasite. The coexistence of all host types (S, P, and H) occurs for intermediate μ, and at high values of μ we observe extinction of the hyperparasite. For all types of trade-off functions, the introduction of the hyperparasite in the system could be beneficial for biological control because numbers of the healthy hosts increase. The dependence of the ESS virulence of the hyperparasitized parasite $\alpha_H(\epsilon)$ on the mortality rate shows an increase with μ in the absence of P and then a decrease when P can coexist with H.

Coevolution of Parasite and Hyperparasite

Now we turn to the joint coevolution of the parasite virulence α and the hyperparasite strength ϵ. In this case, we allowed for coevolution of both the hyperparasite and the parasite. Results (displayed in sec. SM9 of the supplemental PDF) show that the hyperparasite can evolve from a very low hyperparasite effect, $\alpha_0(\epsilon)$, to one that is greater than 1, making the hyperparasite more detrimental to the host than the parasite itself (hypervirulence). However, below we again assume $0 \le \alpha_0(\epsilon) \le 1$ and $0 \le \beta_0(\epsilon) \le 1$; note that in the scenario of hypervirulence it is still possible to observe the coexistence of all model components and the model behavior is not dissimilar to that with hypovirulence.

To study coevolution (with hypovirulence) using an adaptive dynamics framework, we derive the corresponding equations for rare mutants introduced into the resident population. The invasion fitness is given by a system of four differential equations describing the dynamics of hosts

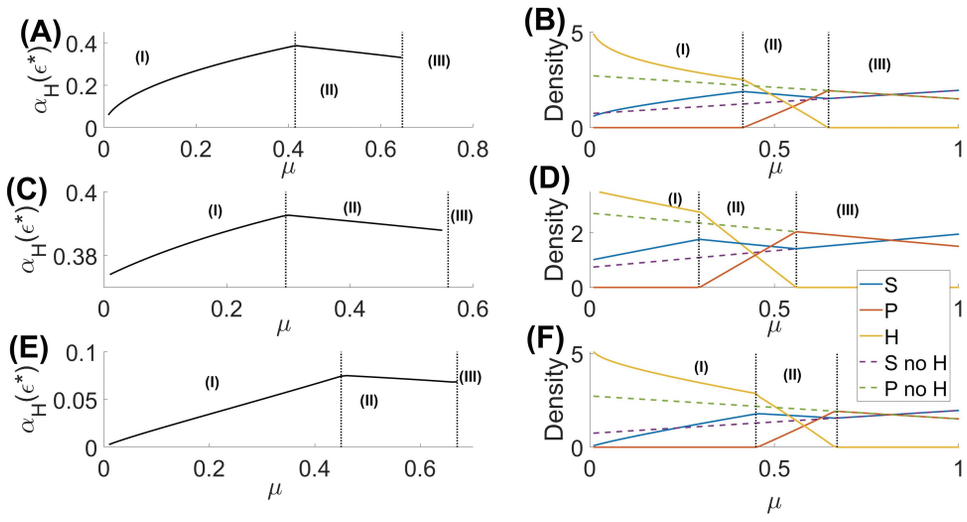

Figure 3: Dependence of the evolutionarily stable strategy (ESS) hyperparasite virulence $\alpha_H(\epsilon^*)$ on background mortality. *A*, *C*, *E*, Hyperparasite virulence at the ESS hyperparasite strength ϵ^* as functions of mortality μ for several trade-off functions: hyperbolic β_0, sigmoidal β_0, and sigmoidal α_0, respectively (see fig. 2). *B*, *D*, *F*, Stationary densities as functions of μ corresponding to the respective ESS plots. Blue curves correspond to healthy susceptible hosts, orange curves correspond to parasitized hosts, yellow curves correspond to hyperparasitized hosts, and dashed purple and green curves represent the stationary densities of susceptible hosts and parasitized hosts, respectively, in the absence of the hyperparasite. Regions I–III are the same as in figure 1. All other parameters are as given in figure 2.

infected by a mutant parasite in the absence of hyperparasite P_m, a mutant parasite in the presence of the resident hyperparasite $H_{m,R}$, a resident parasite in the presence of the mutant hyperparasite $H_{r,M}$, and a mutant parasite in the presence of the mutant hyperparasite $H_{m,M}$. The model equations are provided in appendix C, and the corresponding flowchart is provided in the supplemental PDF. We used analytical methods to analyze the evolutionarily singular points. In particular, we found that eventual evolutionary outcomes are ESSs that are convergent stable; that is, they are evolutionary attractors. We also implemented numerical techniques to simulate the long-term dynamics of the introduction of a rare mutant into a resident equilibrium to determine the winning strain. A typical evolutionary trajectory obtained using the two frameworks is shown in section SM6 of the supplemental PDF. We assumed the same shapes of the corresponding trade-off functions as above for separate evolution of parasite and hyperparasite.

The dependence of the ESS pairs on the background mortality rate μ and the stationary host numbers are shown in figure 4. The results show that in each trade-off scenario, for small values of μ the hyperparasite successfully infects all parasites. In each scenario there exists a range of μ values where all three types of the host can coexist together. Above this range, the hyperparasite becomes extinct, leaving only the susceptible and parasitized hosts. (In effect, increased mortality on the basal resource population, the host, truncates the food chain it supports.) We observe that for most μ values ($0.05 \le \mu \le 1$) the overall mortality in the presence of the hyperparasite is less than (or equal to, when $H^* = 0$) the overall mortality in the absence of the hyperparasite. An interesting observation is that for sigmoidal trade-off scenarios in the absence of P (i.e., when all parasites acquire hyperparasites), their virulence is higher than in the system without hyperparasites. We found that mathematically this fact is related to the shape of the sigmoidal trade-off functions, especially to the magnitude of the curvature.

Interestingly, in some cases coevolution can drive the system to states where either the hyperparasites are extinct ($H_{i,L} = 0$) or there are no parasitized hosts ($P_i = 0$); however, this is not physical extinction of the parasite, as it is always present with the hyperparasite. This is the phenomenon of natural selection forcing the joint species traits to evolve past their respective extinction boundaries, subsequently resulting in the extinction of that species and the end of the evolution of their life-history traits (e.g., in the case of extinction of the hyperparasite). Several studies have demonstrated the occurrence of this counterintuitive outcome (Muir and Howard 1999; Fiegna and Velicer 2003; Parvinen 2005). For example, consider the trade-off scenario with linear $\alpha_0 = \epsilon$ and hyperbolic $\beta_0 = 2\epsilon/(1 + \epsilon)$; depending on the evolutionary starting point and the evolutionary speed, the evolution of both parameters α and ϵ can result in either the parasite virulence or the hyperparasite virulence evolving past their

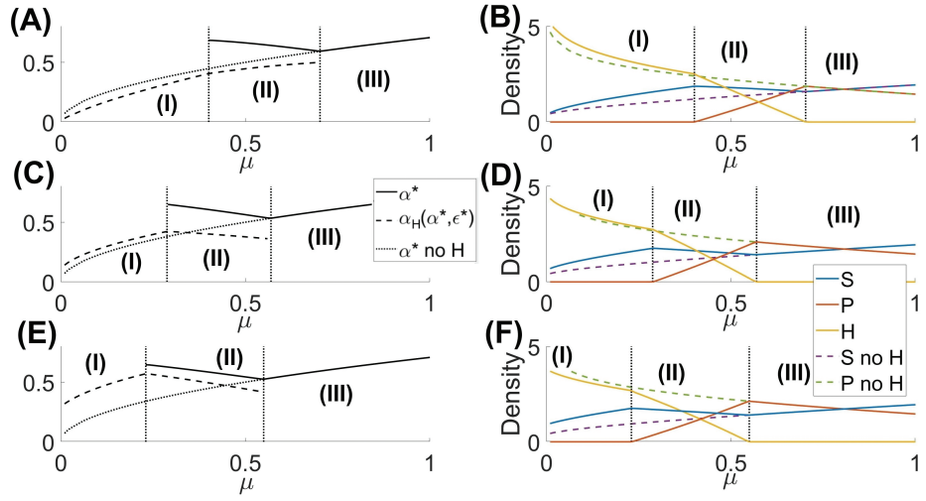

Figure 4: Dependence of the coevolution of parasite virulence and hyperparasite strength on background mortality. *A*, *C*, *E*, Evolutionarily stable strategy (ESS) parasite virulence in the presence of the hyperparasite α^*, the corresponding ESS hyperparasite virulence $\alpha_H(\alpha^*, \epsilon^*)$, and the ESS virulence of the parasite in a system without the hyperparasite for different trade-off combinations: hyperbolic β_0, sigmoidal β_0, and sigmoidal α_0, respectively. *B*, *D*, *F*, Equilibrial densities as functions of μ corresponding to the respective ESS plots, where the densities represented by a dashed line represent the host densities in the absence of the hyperparasite. Regions I–III and line colors are the same as in figure 1. All other parameters are as given in figure 2.

respective extinction boundaries, where only healthy hosts and parasitized hosts persist (i.e., the hyperparasite is extinct, so $H = 0$). An alternative outcome is to have all parasites infected by hyperparasites (i.e., $P = 0$), as shown in figure 5*B*. The figure shows the evolutionary trajectory using the adaptive dynamics framework. (Comparable results emerge using the quantitative genetics framework.) A slower rate of evolution of ϵ can lead to the extinction of the hyperparasite (fig. 5*A*). Which scenario is realized in each case largely depends on the shape of the trade-off functions, which is often hard to measure empirically. We discuss the phenomenon of coevolutionary extinction in more detail in "Discussion" (with an in-depth description of how we can vary the evolutionary speed shown in sec. SM5 of the supplemental PDF).

Another interesting outcome is the possibility of two distinct ESS pairs, with the evolutionary end point being dependent on the initial conditions, that is, evolutionary bistability. Consider the trade-off with α_0 being the sum of two sigmoidal functions and a linear β_0. This can imply that if we start from different initial conditions the system may end up at either low or high evolutionary stable parasite virulence and hyperparasite strength. These two ESS pairs occur as a result of an intermediate range of ϵ values for which the hyperparasite cannot survive in the system; therefore, the hyperparasite strength ϵ evolves away from this range toward either a more virulent or a more benign hyperparasite strain, depending on the initial conditions (for full details, see sec. SM4 of the supplemental PDF).

Effects of Mutual Invasion of Hyperparasites

We have assumed that hyperparasites of different strains do not interact directly. In particular, we assumed that the hyperparasite of strain H_i cannot displace another hyperparasite H_j already established in an individual host. Some previous studies have relaxed this assumption and argued that the possibility of mutual displacement among hyperparasites may result in a different outcome in the evolution of virulence (Taylor et al. 1998; Taylor 2002). In particular, it has been argued that when competing hyperparasites can invade each other via horizontal transmission (superinfection; Alizon et al. 2013), the evolutionarily stable virulence should generally increase. We can assess this conclusion using our framework, which explicitly models the evolution of life-history traits of the parasite and of the hyperparasite.

Consider, for the sake of simplicity, that there is only one parasite type P present but multiple competing hyperparasite strains, denoted by H_i, which we assume to be ordered along an axis so that each strain i competes only with strains $i - 1$ and $i + 1$. Mathematically, we use the same generic model as before; however, in the equation for H_i we add a function G_i:

$$G_i = -\gamma\sigma(\alpha, \epsilon_i)(H_{i-1} + H_{i+1})H_i + \gamma(\sigma(\alpha, \epsilon_{i+1})H_{i+1} + \sigma(\alpha, \epsilon_{i-1})H_{i-1})H_i, \quad (8)$$

where the first term describes the loss in H_i due to invasion and displacement by other strains and the second term

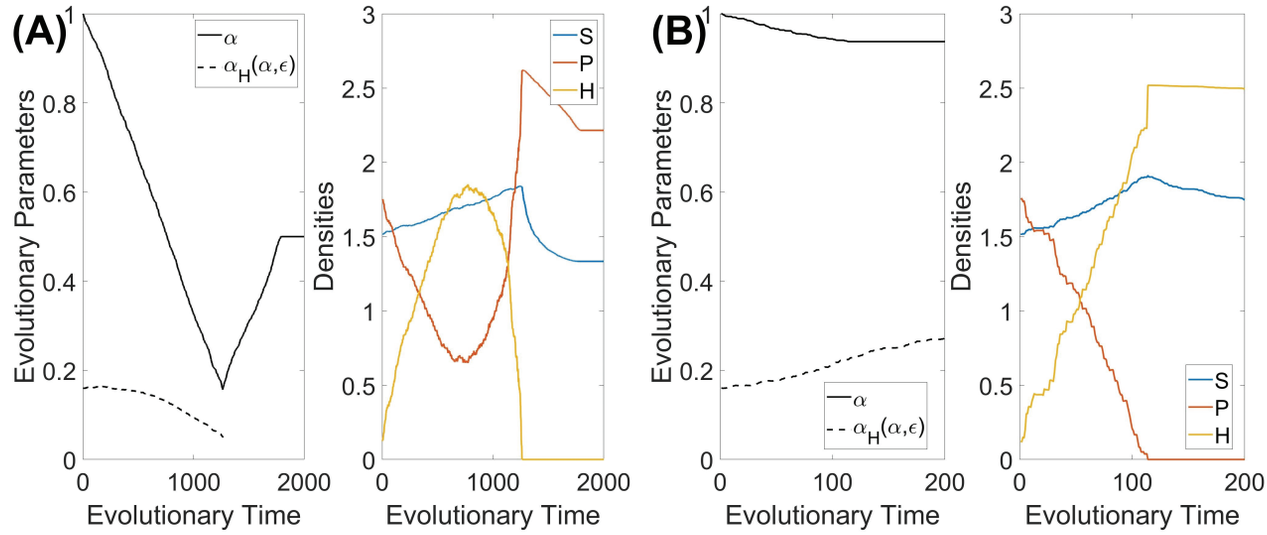

Figure 5: *A*, Example of coevolutionary extinction where the slow coevolution of parasite virulence and hyperparasite strength results in the extinction of the hyperparasite. *B*, Example of an evolutionary outcome where the fast coevolution of parasite virulence and hyperparasite strength results in the disappearance of parasites free of hyperparasites. After the extinction of the parasite, we observe a further decrease in parasite virulence (α) and an increase in hyperparasite virulence $\alpha_H(\alpha, \epsilon)$ until we reach an evolutionarily stable strategy consisting of only *S* and *H*. The left panels show the coevolution of both parasite and hyperparasite virulence simulated through the adaptive dynamics framework, where the solid black curves represent the parasite virulence and the dashed black curves represent the hyperparasite virulence. The right panels show the corresponding equilibrium host densities as life-history traits evolve, with the susceptible host density represented by the blue curve, the parasitized host density represented by the orange curve, and the hyperparasitized host density represented by the yellow curve. All other parameters are as given in figure 2.

accounts for the successful invasion by H_i supplanting other strains. Physically, all displacements of hyperparasite strains occur via transmission in the parasitized host captured by the coefficient $\sigma(\alpha, \epsilon)$. The coefficient γ describes the success of displacement of hyperparasite strains; we vary this coefficient across a wide range. For simplicity, we assume that because of vegetative incompatibility only two hyperparasite strains (H_{i+1} and H_{i-1}) can invade strain H_i. (We should stress that considering a large number of strains that can invade H_i does not crucially affect our main results. More details about the model equations are provided in sec. SM7 of the supplemental PDF.)

Simulation of the modified model shows the possibility of simultaneous coexistence of different hyperparasite strains (see fig. S17). However, the distribution of $H_i(\epsilon)$ has a Gaussian shape with the maximum corresponding to the ESS virulence $\alpha_H(\epsilon^*)$ found in the system with a single hyperparasite strain. Variation of γ, parameterizing the strength of mutual invasions, does not affect the position of the peak. Our general conclusion is that competition of hyperparasites—in the case where we do not allow for multiple infections within individual hosts—does not modify the ESS value of parasite virulence. A major conclusion of early studies was the existence of a positive dependence of the virulence (or transmission rate) on the strength of the horizontal invasion of hyperparasites (Taylor et al. 1998; Taylor 2002). Our results using a more mechanistic model suggest that this does not always hold.

Discussion

Despite an abundant body of theoretical research into evolution and coevolution within host-parasites systems, surprisingly little attention has been paid to systems containing hyperparasites except a few earlier studies (Taylor et al. 1998; Taylor 2002). This is unfortunate given how widespread hyperparasites are in both natural and agricultural populations (Milgroom and Cortesi 2004; Nobrega et al. 2015; Parratt and Laine 2016). Our study partially bridges this gap and theoretically explores possible outcomes of the evolution of parasite virulence in the presence of a hyperparasite. We have presented a novel modeling framework that explicitly describes the evolution of key traits of the parasite along with its hyperparasite. In previous models, it was impossible to separate situations where the virulence of a hyperparasite-infected parasite decreases because of evolution of the parasite itself (i.e., because of changes in parasite life-history traits with a fixed strain of a hyperparasite) from reduced parasite virulence resulting from an increase in the hyperparasite strength debilitating

it (Taylor et al. 1998; Taylor 2002). Our framework allows us to discriminate these scenarios. Mathematically, we have utilized two powerful approaches for modeling biological evolution—adaptive dynamics (Geritz et al. 1997; Brännström et al. 2013) and quantitative genetics (Abrams et al. 1993*a*; Day and Proulx 2004)—and found that they reached comparable conclusions about the evolution of virulence in tritrophic systems. Note that our framework partly includes effects of genotype-to-genotype interactions, which are considered to be crucial for parasite-hyperparasite coevolution (Parratt et al. 2017). For example, the hyperparasite strain characterized by ϵ has different effects on its parasite depending on α, which are described by the overall virulence and the transmission rates given by $\alpha_H(\alpha, \epsilon)$, $\beta_H(\alpha, \epsilon)$, and $\sigma(\alpha, \epsilon)$. Genetic incompatibility was assumed in the model when exploring effects of mutual invasion of the hyperparasite (see the corresponding section). Note as well that for simplicity we do not account for independent transmission of hyperparasites among parasite populations. Neither do we allow for recovery of either parasitized or hyperparasitized hosts to their uninfected states (both of these scenarios can be explored by extending the current model).

Our major insights are as follows. First, we have shown that introducing a hyperparasite generally increases parasite virulence. We need to take this into account in virulence management programs. Second, we have compared host population sizes and infection prevalence in the presence and absence of the hyperparasite. Typically, our results suggest that the introduction of a hyperparasite as a biocontrol agent should be beneficial for the system, for example, as measured in terms of overall host mortality and the equilibrium number of healthy hosts. Third, we have shown the possibility of extinction arising because of evolution in the coevolving system. Finally, we have demonstrated examples of evolutionary bistability: starting from different initial conditions the evolutionarily stable virulence can be either low or high. Below we discuss the significance of these insights and reflect on possible biological applications.

Applications to Biological Control

Hyperparasites can be a nuisance if they debilitate biological control agents (Beddington and Hammond 1977). But they can also be a potentially powerful biological control tool in ecology, agriculture, and medicine that reduces the burden of parasites (Abo-Foul et al. 1996; Swinton and Gilligan 1999; Milgroom and Cortesi 2004; Nobrega et al. 2015). One particularly salient and important case of the potential biocontrol of a parasite by its obligate hyperparasite is the attenuation of the devastating impact of chestnut blight disease by a hypovirus (Milgroom and Cortesi 2004). Chestnut blight disease is caused by the fungus *Cryphonectria parasitica*. The fungus was introduced in the United States around 1904 and devastated the American chestnut (*Castanea dentata*) across its range during the first half of the twentieth century, and its negative impact is still ongoing (Taylor et al. 1998; Milgroom and Cortesi 2004). The total estimated loss across the continent was about 3.5 billion trees (Anagnostakis 1982). By contrast, in Europe the invasion of the chestnut blight fungus (first reported in 1938) resulted in only very low mortality of infected trees of the European chestnut (*Castanea sativa*; Heiniger and Rigling 1994; Ghabrial and Suzuki 2009). The mild loss of chestnut trees in Europe appears to be explained by the debilitating effects of the pathogen of a virus, *Cryphonecria hypovirus 1* (a naked double-stranded ribonucleic acid molecule). Given the successful natural biological control of the disease in Europe, several management programs have been proposed involving inoculation of infected chestnut trees with the hypovirus in the United States. However, treatment with the hypovirus has not yet been particularly successful in the United States, at least as assessed by reducing tree mortality (Milgroom and Cortesi 2004).

Various reasons have been suggested to explain the failure of biological control of chestnut blight disease. High diversity of vegetative compatibility of the fungus (i.e., the fact that a particular viral strain can infect only a particular type of fungus) may explain the biocontrol failure (Milgroom and Cortesi 2004). Another reason may be a low horizontal transmission rate of the hyperparasite due to a low density of host trees. Different strains of *Cryphonecria hypovirus* with different transmission rates exist. Such heterogeneity could explain variability in the success of establishment among trials (Morozov et al. 2007). In our model, this is described by altering the parameter β_0 (see fig. S8). Evolution within hyperparasites toward dominance by less debilitating viral strains has been suggested to play a role (Taylor et al. 1998; Taylor 2002). Earlier models suggested the hypovirus would evolve to minimize its deleterious effect on the parasite. It is possible that the initial success story of the recovery of chestnut trees in Europe that was ascribed to impacts of the hyperparasite might be evolutionarily unstable or simply a transient phase (Taylor 2002). If so, we should expect a further gradual intensification of the disease in Europe in future years, as a result of the coevolution of the parasite and the hyperparasite.

Our study predicts that in the presence of a hyperparasite, the virulence of the uninfected parasite should increase (see theorem 1). An increase in parasite virulence is observed both for the evolution of the parasite or the hyperparasite alone and for their joint coevolution. This contributes to the long-standing debate about shifts in the parasite virulence in the presence of a hyperparasite (Parratt and Laine 2016). For example, the existing definition

of hypovirulence as a reduction in observed pathogen virulence in the presence of a hyperparasite (Parratt and Laine 2016) may require clarification, since long-term coevolution may increase the observed virulence even if the pathogen's own well-being is negatively affected. In our model, the ESS for parasite virulence positively depends on its rate of loss, in particular on the background mortality (see the end of app. A). Thus, adding some extra loss of parasitized hosts would require higher values of virulence to compensate for the effects of loss. (A similar mechanism leading to increased virulence was reported when adding an external predator to a host-parasite system; Morozov and Adamson 2011; Morozov and Best 2012). On the other hand, the model shows that despite the increase in virulence of the parasite, the introduction of a hyperparasite over most of the parameter space should be beneficial for biological control. For example, the number of healthy hosts at the evolutionarily stable parasite virulence is higher compared with the hyperparasite-free case (cf. figs. 2, 4). This occurs because of the redistribution of infected hosts from the compartments parasitized to hyperparasitized, and mortality of the latter is lower. Although we could not prove this fact analytically, we numerically observed the beneficial effects of biological control by a hyperparasite for any set of parameters for which susceptible hosts, parasites, and hyperparasites can coexist.

Along with the chestnut blight disease case study, our system and results can potentially be applied to other empirical examples. For example, the interaction between the powdery mildew pathogen and its obligate hyperparasite *Ampelomyces quisqualis* is characterized by a fast parasite-hyperparasite coevolution and a high prevalence of hyperparasitism (Parratt et al. 2017). For this system, our model might predict a further increase in the prevalence of hyperparasites with an increase in the virulence of the pathogen (see fig. 5*B*). However, for more accurate predictions of this system, one needs to incorporate the effects of genotype-to-genotype match and spatial aspects of the problem (Parratt et al. 2017). Another interesting biological application is the system consisting of ants (hosts), their parasitic fungus *Ophiocordyceps* spp., and a fungal hyperparasite, which exhibits complex population-level feedback (Andersen et al. 2012). Conceptually, the role of the hyperparasite in reducing the impact the parasite has on the host in the given system is arguably similar to the one predicted in the model. In particular, it was observed that although the hyperparasite reduces the number of successful infections of the parasite at the individual level (i.e., debilitating the parasitic fungus), overall the persistence of the fungal infection becomes facilitated, that is, the effective pathogen virulence increases (Andersen et al. 2012). The next possible practical application from our theoretical modeling comes from the example of coevolutionary extinction: the use of phages as a therapy can be counterproductive, since genetic variation in the phage evolution may result in the eventual disappearance of hyperparasites (phages) with a higher prevalence of parasites (e.g., fig. 5*A*).

Unlike results reported in earlier literature, we find that the evolution of the hyperparasite alone or its joint coevolution with the parasite can result in evolution toward some intermediate values of hyperparasite strength (see figs. 3, 4). For the chestnut blight control study case in Europe, this suggests that the hypovirus should not necessarily evolve to minimize its impact on the parasite, as predicted previously (Taylor et al. 1998; Taylor 2002). Combined with the outcome of our model predicting increased host numbers in the system with a hyperparasite, this study provides us with a theoretical basis to be optimistic about the use of a hypovirus as a biological control agent against the parasitic fungus *C. parasitica* and similar systems, provided our assumptions about the shape of trade-off functions are correct. On the other hand, the effects of coevolutionary extinction—when a gradual improvement of evolutionary fitness results in the eventual extinction of a species—can also affect the results of biological control. This phenomenon mostly has been reported in theoretical studies; however, some empirical studies exist that confirm the possibility of coevolutionary extinction (see Travisano 1997; Muir and Howard 1999).

Coevolutionary Extinction in Systems with Hyperparasitism

Our study shows the possibility of a coevolutionary extinction in the system, that is, the situation where a gradual adaptation of a life-history trait eventually results in population extinction. The phenomenon of evolutionary suicide has been observed in other theoretical studies (Matsuda and Abrams 1994; Muir and Howard 1999; Fiegna and Velicer 2003), and a brief classification of possible scenarios has been proposed (Webb 2003; Parvinen 2005). In our system, the most interesting scenario includes a coevolutionary extinction that depends on the rates of mutation of the life-history traits of the parasite and hyperparasite (see fig. 5). Coevolutionary extinction occurs with simple Monod-like trade-off relations (Monod 1949; see figure captions) between the virulence and transmission rates (transmission is proportional to virulence for low virulence but saturates and approaches a constant value at high virulence).

In the model, slow mutation rates lead to a gradual decrease in the virulence of both hyperparasite-free parasites and parasites containing hyperparasites (fig. 5*A*). The decrease in parasite virulence (and the corresponding transmission rate) initially results in a lower number

of parasitized hosts, which signifies successful biological control. However, a further decrease in α and α_H results in a drop of H, since transmission rates of hyperparasites become too low to allow the hyperparasite to persist and thus the hyperparasite becomes extinct. In the absence of the hyperparasites, parasites then evolve to their ESS virulence. Interestingly, extinction of hyperparasites occurs in the model via a transcritical rather than a saddle-node bifurcation (see the supplemental PDF), which has been previously considered an unfavorable condition for evolutionary suicide (Parvinen 2005). For fast mutation rates (fig. 5*B*), the virulence of parasites containing hyperparasites α_H quickly increases, whereas the virulence of hyperparasite-free parasites α decreases. This discrepancy can be explained by a rapid increase in the hyperparasite strength measured by ϵ. As a result, the hyperparasites wins their competition with the parasites for the same resources, the susceptible hosts. The eventual outcome of evolution is the coexistence of the susceptible and hyperparasitized hosts; however, from a biological point of view there is no true coevolutionary extinction, since both parasite and hyperparasite remain in the system.

Mathematically, the dependence of coevolutionary outcomes on the mutation rates can be explained by the fact that the boundary stationary states (either in the absence of hyperparasitized hosts or in the absence of parasitized hosts) are globally stable in some domains of the evolving parameters α and ϵ. Thus, if with time the evolutionary trajectory lands in the domains of stability of either of the boundary stationary states, this will signify a quick extinction of the third component (hyperparasitized hosts or parasitized hosts, respectively). Moreover, if for each resultant two-component subsystem an ESS occurs in the domain of stability of the boundary stationary state (the third component is zero), the system will be trapped in the given evolutionary state.

From a disease management perspective, the possibility of coevolutionary extinction—which would depend on how fast mutations happen—adds an extra degree of uncertainty in forecasting eventual evolutionary outcomes. Indeed, for a time series of eco-evolutionary dynamics (as those in fig. 5) it is hard to predict the final evolutionary outcome from early dynamics: the initial success of biological control of chestnut blight disease by a hypovirus in Europe reported in Heiniger and Rigling (1994) could, for instance, be a transient phenomenon, as shown in figure 5*A*. Considering that the chestnut blight–hypovirus interaction example poses the fundamental (and nontrivial) question about timescales as to whether we should separate evolutionary and ecological processes in this or similar cases studies. The generation time of chestnut trees (50–70 years) is much longer than that of the fungus and is especially longer than the replication time of a hypovirus (hours), which governs mutation rates (Abo-Foul et al. 1996; Swinton and Gilligan 1999; Milgroom and Cortesi 2004; Nobrega et al. 2015). In this case, proposed classifications of types of coevolutionary extinction using the classical adaptive dynamics framework assuming the ecological scale to be fast relative to evolution (e.g., Parvinen 2005 and references therein) should be reconsidered. The evolutionary outcome may be highly sensitive to the choice of the mathematical formulation of trade-off relations (assuming that such trade-offs exist), and for a given parameterization (Monod function) it can largely depend on the values of parameters. For example, using the Monod dependence of $\beta_0(\epsilon)$ for some parameters different from those in figure 5 demonstrates the possibility of an internal ESS where all components—susceptible, parasitized, and hyperparasitized hosts—coexist (see fig. 4 and examples in the supplemental PDF).

Future Development of Theory and Empirical Observation

This study should be regarded as a first step in exploring the evolution of virulence in tritrophic host-parasite systems based on a mechanistic approach. We have made several simplified assumptions, which could be relaxed in further studies. In particular, we have neglected the effect of coinfections, that is, the coexistence of several strains of a parasite within a single host. Accounting for coinfections may potentially increase the virulence of an individual parasite strain as well as the overall "average" virulence as a result of competition among strains within individual hosts (Alizon and van Baalen 2008; Alizon et al. 2013). Another important source of complexity warranting further study is the effects of vegetative incompatibility, that is, where a genetic barrier prevents a particular hyperparasite from infecting different varieties of the parasite that are incompatible with that hyperparasite (Carbone et al. 2004; Milgroom and Cortesi 2004). Although some mathematical models have included effects of vegetative incompatibility in systems with hyperparasites (Liu et al. 2000), the evolutionary aspects of this issue have not been addressed. Our modeling framework can be easily extended to explore evolutionary effects of vegetative incompatibility. For example, we could introduce weights $w_{i,j}$ in the transmission term $w_{i,j}\sigma(\alpha_i, \epsilon_L)H_{i,L}P_j$ (and similar terms) such that for parasite strain i with a largely different genetic composition than strain j, transmission of the hyperparasite would hardly be possible—that is, $w_{i,j} \ll 1$. Including genetic incompatibility and, in general, genotype × genotype effects in the model will allow us to explore some other empirical systems (Swinton and Gilligan 1999; Kiss et al. 2004; Milgroom and Cortesi 2004; Nobrega et al. 2015; Parratt et al. 2017).

Another important direction is a more rigorous investigation of the implications of the form and parameter values of trade-off functions between virulence and transmission. Our study demonstrates that the model prediction about the coexistence of both parasitized hosts and hyperparasitized hosts as well as the ESS value of virulence depend crucially on the shape of $\beta(\alpha)$, $\alpha_0(\epsilon)$, and $\beta_0(\epsilon)$. This contingency is often considered a bugbear in the forecasting of evolutionary outcomes (Kisdi et al. 2013). Empirical data clarifying the shape of the transmission-virulence trade-off would be of great value. However, relevant data are scarce and do not allow one to discriminate between different mathematical formulations of trade-off functions. In many cases, available data reveal only that pathogen transmission is an increasing and saturating function of virulence (de Roode et al. 2008; Alizon et al. 2009). In particular, a more accurate reconstruction of trade-off functions will be crucial to assess the plausibility of evolutionary bistability predicted by our model (see sec. SM4 of the supplemental PDF). The reported scenario for stability requires the sign of the curvature to change multiple times (i.e., something similar to an s-shaped trade-off). This may not be all that likely biologically.

Throughout this article, we have assumed that the main beneficial effect of hyperparasites is the reduction of virulence of the parasite, that is, $\alpha > \alpha_H$. However, it has been reported in several systems that hyperparasites can enhance recovery of the basal host (Morozov et al. 2007; Parratt and Laine 2016). Mathematically, allowing for a hyperparasite-mediated recovery requires adding an extra negative term to the equation for hyperparasitized hosts (and a corresponding positive term in the equation for susceptible hosts), which can potentially modify the evolution of both the parasite and the hyperparasite. Another unexplored issue is the positive impact of the hyperparasite on host resistance, which can enhance recovery, reduce host mortality, and diminish transmission of the hyperparasite. Conventional wisdom predicts that evolution of the hyperparasite traits should minimize (eventually to zero) their detrimental effects on the parasite (Parratt and Laine 2016). Our modeling approach can be used to reevaluate this conventional wisdom.

Among other unexplored issues are the following. First, it is important to empirically verify our main conclusion about an evolutionary increase in the virulence of the uninfected parasite due to the presence of the hyperparasite. An empirical example confirms that the presence of a hyperparasite can strengthen the persistence of the parasite (Andersen et al. 2012). However, to the best of our knowledge, a thorough comparison of parasite virulence before and after the establishment of a hyperparasite (allowing sufficient time for evolution) has not yet been done. Second, spatial heterogeneity can affect the success of disease transmission and evolution (Swinton and Gilligan 1999; Parratt et al. 2017; Lion 2018; Liu et al. 2000). Incorporating spatial structure can have many important and at times surprising effects on eco-evolutionary dynamics. Third, the influence of initial conditions in systems with hyperparasitism has been explored in previous studies (Taylor et al. 1998; Morozov et al. 2007); however, the evolutionary implications of initial conditions have not been elucidated. Finally, it will be important to address the sensitivity of all of our predictions to the choice of the functional form of disease transmission. In this study, we have assumed this functional form to be that of mass action, a density-dependent process (McCallum et al. 2001). Alternative functional forms for transmission (e.g., Ponciano and Capistrán 2011) could imply different evolutionary outcomes. All of these issues are ripe for future theoretical exploration and will be important to understand if one is to effectively use hyperparasites in the biological control of parasites of economic and societal importance.

Our analyses have examined the evolution and coevolution of parasites and hyperparasites, but in many systems hosts would be expected to evolve as well, for instance via traits that confer resistance to transmission of a pathogen or tolerance once infected. In some cases, one could envisage that changes in host traits would alter the trade-off functions faced by evolving parasites and hyperparasites, shifting how they evolve; this in turn could alter the direction of selection on host traits. Future theoretical analyses of evolution in a tritrophic context should help unravel the potentially surprising eco-evolutionary consequences of such feedbacks. Abdala-Roberts et al. (2019) recently argued that a consideration of tritrophic interactions is important for understanding a wide range of patterns in communities and ecosystems, and they note that "from an evolutionary standpoint, few studies have explicitly tested how natural selection on species traits acts within [tritrophic interactions]" (p. 2156). We suspect that the interaction among hosts, parasites, and hyperparasites may prove to be a particularly important and as yet still poorly studied arena within which evolution impacts ecological processes. The models and results we have here presented provide, we believe, the first step toward a deeper understanding of this complex yet ubiquitous pattern of interactions.

Acknowledgments

We appreciate helpful suggestions made by Associate Editor Michael H. Cortez as well as by two anonymous reviewers. R.D.H. and M.B. acknowledge support from the University of Florida Foundation and from US Department of Agriculture grant 2017-67013-26870 as part of the joint USDA-NSF-NIH Ecology and Evolution of Infectious Diseases program.

Statement of Authorship

A.Y.M. and R.D.H. conceptualized the presented idea. A.Y.M. and M.B. developed the model. S.K.S. conducted all coding and performed all numerical simulations under the supervision of A.Y.M. S.K.S., A.Y.M., and M.B. conducted all model analysis. S.K.S., A.Y.M., and R.D.H. wrote the original draft with all authors contributing to the review and editing of the draft. All authors provided crucial feedback and helped shape the research, analysis, and manuscript.

APPENDIX A

Here, we derive the invasion fitness for evolution in the parasite. Consider equations (4) and (5) for mutant dynamics. Because the upper right element of the Jacobian is zero, its eigenvalues are the diagonal elements, which are

$$\begin{cases} \lambda_P = \beta_P(\alpha_m)S^* - \sigma(\alpha_r)H_r^* - \mu - \alpha_m, \\ \lambda_H = \beta_H(\alpha_m)S^* + (1-Q)\sigma(\alpha_m)P_r^* - \mu - \alpha_H(\alpha_m). \end{cases}$$

The invasion fitness is determined by $\max(\lambda_H, \lambda_P)$. However, under the assumption that we only allow for small mutations (i.e., α_m is close to α_r), we can consider λ_P as invasion fitness. Indeed, along the line $\alpha_r = \alpha_m$ from $0 = dH/dt$, we have $H_r^*(\lambda_H + Q\sigma(\alpha_r)P_r^*) = 0$, from which it follows that $\lambda_H = -Q\sigma(\alpha_r)P_r^* < 0$. Because of the differentiability of the functions (we assume the trade-off functions to be differentiable as well), there exists a nonzero measure band along the line $\alpha_r = \alpha_m$ such that $\lambda_H < 0$, so we can consider λ_P to be the invasion fitness for the purpose of determining evolutionarily singular points, which are always located on $\alpha_r = \alpha_m$:

$$\lambda_P' = \beta_P'(\alpha^*)S^* - 1 = 0.$$

By finding the values of α^* such that this expression is satisfied, we are able to locate any singular points. Using the principles of adaptive dynamics (Geritz et al. 1997; Brännström et al. 2013), we are able to determine the stability of these points. Assuming that β_P is a concave function of α,

$$E = \frac{\partial^2 \lambda_P}{\partial \alpha_m^2} = \beta_P''(\alpha^*)S^* < 0,$$

$$M = \frac{\partial^2 \lambda_P}{\partial \alpha_m \partial \alpha_r} = \beta_P'(\alpha^*)\frac{\partial S^*}{\partial \alpha_r}.$$

Hence, because $E < 0$ and $E + M = \beta_P''(\alpha^*)S^* + \beta_P'(\alpha^*)\partial S^*/\partial \alpha_r < 0$ (in some cases this can be proven analytically and in others computationally; for more details, see sec. SM8 of the supplemental PDF), all singular points will be both evolutionarily and convergence stable; hence, all singular points will be an ESS.

APPENDIX B

Here, we prove theorem 1, determining the impact of the hyperparasite on the ESS.

First consider the case of no hyperparasites; that is, set $H = 0$ in the model equations. From this host-parasite model, the invasion fitness of a mutant pathogen into a population with one resident pathogen can be found by following the adaptive framework:

$$\lambda = \beta_P(\alpha_m)\hat{S} - \mu - \alpha_m,$$

where $\hat{S}$ is the equilibrium S in the resident population and α_m is the mutant virulence. From this we can find the fitness gradient:

$$\Rightarrow \lambda' = \beta_P'(\alpha_m)\hat{S} - 1.$$

At the ESS, denoted as $\hat{\alpha}$, the invasion fitness and selection gradient vanishes; that is, $\lambda = 0$ and $\lambda' = 0$:

$$0 = \lambda = \beta_P(\hat{\alpha})\hat{S} - \mu - \hat{\alpha}, \tag{B1}$$

$$0 = \lambda' = \beta_P'(\hat{\alpha})\hat{S} - 1. \tag{B2}$$

Using equation (B2), it is possible to derive an expression for the susceptible host stationary state $\hat{S}$ at the ESS:

$$\Rightarrow \hat{S} = \frac{1}{\beta_P'(\hat{\alpha})}.$$

Substitution of this into equation (B1) allows an expression dependent only on $\hat{\alpha}$ to be found:

$$\Rightarrow \frac{\beta_P(\hat{\alpha})}{\beta_P'(\hat{\alpha})} - \hat{\alpha} = \mu. \tag{B3}$$

Now we can return to the case of the host-parasite-hyperparasite model. Using the adaptive dynamics framework (under the assumption that mutations occur in small steps and therefore λ_H is always negative), the ESS, α^*, is given when $\lambda_P = 0$ and $\lambda_P' = 0$, where

$$\lambda_P = 0 = \beta_P(\alpha^*)S^* - \sigma(\alpha^*)H^* - \mu - \alpha^*, \tag{B4}$$

$$\lambda_P' = 0 = \beta_P'(\alpha^*)S^* - 1, \tag{B5}$$

and S^* and H^* are the resident equilibria for a system with a single pathogen and hyperparasite. Using this equation, it is again possible to derive an expression for the host stationary state S^*:

$$\Rightarrow S^* = \frac{1}{\beta_P'(\alpha^*)}.$$

Again, the substitution of this into equation (B4) yields an expression dependent only on α^*:

$$\Rightarrow \frac{\beta_P(\alpha^*)}{\beta'_P(\alpha^*)} - \alpha^* = \mu + \sigma(\alpha^*)H^* \geq \mu. \tag{B6}$$

Using both expression (B3) and expression (B6), it is possible to derive a relationship between α^* and $\hat{\alpha}$:

$$\Rightarrow \frac{\beta_P(\alpha^*)}{\beta'_P(\alpha^*)} - \alpha^* \geq \frac{\beta_P(\hat{\alpha})}{\beta'_P(\hat{\alpha})} - \hat{\alpha}.$$

Assuming that $\beta_P(\alpha)$ is an increasing function with a negative second derivative, we can determine the derivative of the function $\beta_P(\alpha)/\beta'_P(\alpha) - \alpha$ with respect to α as

$$\left(\frac{\beta_P(\alpha)}{\beta'_P(\alpha)} - \alpha\right)' = \frac{\beta'_P(\alpha)\beta'_P(\alpha) - \beta_P(\alpha)\beta''_P(\alpha)}{(\beta'_P(\alpha))^2} - 1$$

$$\Rightarrow \left(\frac{\beta_P(\alpha)}{\beta'_P(\alpha)} - \alpha\right)' = 1 - \frac{\beta_P(\alpha)\beta''_P(\alpha)}{(\beta'_P(\alpha))^2} - 1 = -\frac{\beta_P(\alpha)\beta''_P(\alpha)}{(\beta'_P(\alpha))^2} \geq 0.$$

From this $\beta_P(\alpha)/\beta'_P(\alpha) - \alpha$ can be defined as an increasing function; therefore, it follows that

$$\Rightarrow \alpha^* \geq \hat{\alpha}.$$

Furthermore, as $1/\beta'_P(\alpha)$ is an increasing function ($(1/\beta'_P(\alpha))' = -\beta''_P(\alpha)/(\beta'_P(\alpha))^2 \geq 0$) and given that $\alpha^* \geq \hat{\alpha}$, it is clear that $1/\beta'_P(\alpha^*) \geq 1/\hat{\alpha}$ and therefore

$$\Rightarrow S^* \geq \hat{S}. \tag{B7}$$

This implies that the equilibrium density for uninfected susceptible hosts is higher in the presence of the hyperparasite, and therefore the introduction of the hyperparasite can be beneficial to the hosts.

We can also consider the scenario in the absence of the hyperparasite-free parasitized hosts with $P = 0$, assuming that $\beta_H = \beta_0\beta_P$. Using the adaptive dynamics framework, the ESS, α^*, is given when $\lambda_H = 0$ and $\lambda'_H = 0$, where

$$\lambda_H = 0 = \beta_H(\alpha^*)S^* - \mu - \alpha_H(\alpha^*),$$
$$\lambda'_H = 0 = \beta'_H(\alpha^*)S^* - \alpha'_H(\alpha^*) = \beta_0\beta'_P(\alpha^*)S^* - \alpha_0,$$

and S^* is the resident equilibrium for a system with no hyperparasite-free pathogens and a single strain of hyperparasite. Using this equation it is again possible to derive an expression for the host stationary state S^*:

$$\Rightarrow S^* = \frac{\alpha_0}{\beta_0\beta'_P(\alpha^*)}.$$

Again, the substitution of this into the equation for λ_H yields an expression dependent only on α^*:

$$\Rightarrow \frac{\beta_P(\alpha^*)}{\beta'_P(\alpha^*)} - \alpha^* = \frac{\mu}{\alpha_0} \geq \mu. \tag{B8}$$

This is similar to expression (B6) and therefore the same result follows, so the theorem is satisfied in this case as well. However, note that in this case all infected hosts have virulence α^*_H.

Note that in all simulations and results we have reported, a hyperbolic trade-off function is considered; that is, $\beta_P(\alpha) = C\alpha/(K + \alpha)$, where C and K are constants. In this case, the expression for the ESS is given as $(\alpha^*)^2 = K(\sigma(\alpha^*)H^* + \mu)$ when both P and H are present, $(\alpha^*)^2 = K\mu$ when only P is present, and $(\alpha^*)^2 = K\mu/\alpha_0$ when only H is present.

APPENDIX C

Here, we provide details on the implementation of the adaptive dynamics framework to modeling the coevolution of a parasite and a hyperparasite. The dynamics of the invading mutant strains are described by the following equations:

$$\begin{aligned}
\frac{dP_m}{dt} &= \beta_P(\alpha_m)S^*P_m - \sigma(\alpha_r, \epsilon_R)P_mH^*_{rR} \\
&\quad - \mu P_m - \alpha_m P_m, \\
\frac{dH_{rM}}{dt} &= \beta_H(\alpha_r, \epsilon_M)S^*H_{rM} + P\sigma(\alpha_m, \epsilon_M)P^*_rH_{mM} \\
&\quad + \sigma(\alpha_r, \epsilon_M)P^*_rH_{rM} - \mu H_{rM} - \alpha_H(\alpha_r, \epsilon_M)H_{rM}, \\
\frac{dH_{mM}}{dt} &= \beta_H(\alpha_m, \epsilon_M)S^*H_{mM} + (1 - Q)\sigma(\alpha_m, \epsilon_M)P^*_rH_{mM} \\
&\quad - \mu H_{mM} - \alpha_H(\alpha_m, \epsilon_M)H_{mM}, \\
\frac{dH_{mR}}{dt} &= \beta_H(\alpha_m, \epsilon_R)S^*H_{mR} + Q\sigma(\alpha_r, \epsilon_R)P_mH^*_{rR} \\
&\quad + (1 - Q)\sigma(\alpha_m, \epsilon_R)P^*_rH_{mR} - \mu H_{mR} \\
&\quad - \alpha_H(\alpha_m, \epsilon_R)H_{mR},
\end{aligned}$$

where S^*, P^*_r, and H^*_{rR} are the stationary states for the resident system with parasite virulence α_r and hyperparasite strength ϵ_R and with H_{iJ} representing the hyperparasite with parasite virulence α_i and hyperparasite strength ϵ_J.

To analytically derive the equations for evolutionarily singular points and verify their stability, we can use the following expressions of invasion fitness obtained for the cases of evolution of parasites and hyperparasites (see the main text and app. A). They read as

$$\begin{aligned}
\lambda_P &= \beta_P(\alpha_m)S^* - \sigma(\alpha_r, \epsilon_R)H^*_{rR} - \mu - \alpha_m, \\
\lambda_{H_{rM}} &= \beta_H(\alpha_r, \epsilon_M)S^* + \sigma(\alpha_r, \epsilon_M)P^*_r - \mu - \alpha_H(\alpha_r, \epsilon_M).
\end{aligned}$$

Note that there are actually four possible eigenvalues of the system, λ_P, $\lambda_{H_{rM}}$, $\lambda_{H_{mM}}$, and $\lambda_{H_{mR}}$; however, on the

manifold given by $(\alpha_r, \epsilon_R) = (\alpha_m, \epsilon_M)$, we have $\lambda_{H_{mM}} = \lambda_{H_{mR}} = \lambda_{H_{rM}} - Q\sigma(\alpha_r, \epsilon_R)P_r^* < \lambda_{H_{rM}}$. As all functions are differentiable, it follows that we have a nonzero measure band along the set $\alpha_r = \alpha_m$, $\varepsilon_R = \varepsilon_M$ (i.e., when we consider small mutational steps in both α and ϵ), such that $\lambda_{H_{mM}}, \lambda_{H_{mR}} < \lambda_{H_{rM}}$. Therefore, the two eigenvalues λ_P and $\lambda_{H_{rM}}$ are sufficient in determining any ESS points. To find any singular points, we need to locate the pairs (α^*, ϵ^*) such that $\lambda'_P = \lambda'_{H_{rM}} = 0$. This is the same condition for the stationary states of the genetic model (app. D), meaning that the two techniques are equivalent. We implement the analytical criteria described in Matessi and Di Pasquale (1996):

$$E_1 = \frac{\partial^2 \lambda_P}{\partial \alpha_m^2} = \beta_P''(\alpha^*)S^* < 0,$$

$$M_1 = \frac{\partial^2 \lambda_P}{\partial \alpha_m \partial \alpha_r} = \beta_P'(\alpha^*)\frac{\partial S^*}{\partial \alpha_r},$$

$$E_2 = \frac{\partial^2 \lambda_{H_{rM}}}{\partial \epsilon_M^2} = \beta_0''(\epsilon^*)\beta_P(\alpha^*)(S^* + \sigma_0 P_r^*) - \alpha_0''(\epsilon^*)\alpha^*,$$

$$M_2 = \frac{\partial^2 \lambda_{H_{rM}}}{\partial \epsilon_M \partial \epsilon_R} = \beta_0'(\epsilon)\beta_P(\alpha)\left(\frac{\partial S^*}{\partial \epsilon_r} + \sigma_0 \frac{\partial P^*}{\partial \epsilon_r}\right).$$

We have ESS stability, as $E_i < 0$; we also have "isoclinic stability," as $E_i + M_i < 0$ (for more details, see sec. SM8 of the supplemental PDF). Furthermore, along with isoclinic stability, another condition must be met to ensure absolute convergence stability (Kisdi 2006):

$$\left| \frac{\partial^2 \lambda_P}{\partial \epsilon_R \partial \alpha_m} \frac{\partial^2 \lambda_{H_{rM}}}{\partial \alpha_R \partial \epsilon_m} \right| - (E_1 + M_1)(E_2 + M_2) < 0.$$

This is shown to always be true in section SM8 of the supplemental PDF. Therefore, if for a particular trade-off combination there is a stable ESS for evolution in the hyperparasite, only then will there exist a corresponding ESS given evolution in both the parasite and the hyperparasite. Furthermore, any singularity will be either an evolutionary attractor (ESS) or an evolutionary repeller, meaning that branching can never occur.

APPENDIX D

Here, we provide the equations for the species densities and life-history traits modified from model (1)–(3) utilized within the quantitative genetics framework (Abrams et al. 1993*a*; Day and Proulx 2004):

$$\frac{dS}{dt} = F(N)S - \mu S - (\beta_P(\alpha)SP + \beta_H(\alpha, \epsilon)SH), \quad \text{(D1)}$$

$$\frac{dP}{dt} = (\beta_P(\alpha)S - \sigma(\alpha, \epsilon)H - \mu - \alpha)P, \quad \text{(D2)}$$

$$\frac{dH}{dt} = (\beta_H(\alpha, \epsilon)S + \sigma(\alpha, \epsilon)P - \mu - \alpha_H(\alpha, \epsilon))H, \quad \text{(D3)}$$

$$\frac{d\alpha}{dt} = G_\alpha \frac{\partial r_P}{\partial \alpha}, \quad \text{(D4)}$$

$$\frac{d\epsilon}{dt} = G_\epsilon \frac{\partial r_H}{\partial \epsilon}. \quad \text{(D5)}$$

The quantities G_α and G_ϵ are the constant genetic variations of α and ϵ, respectively, where mutation replenishes genetic variation (not directly modeled). The terms r_P and r_H describe, respectively, the per capita growth rate of the parasite and the hyperparasite (the expressions for λ_P and λ_H are derived in "Results" and the appendixes). Unlike the classical quantitative genetics framework (e.g., Abrams et al. 1993*a*; Day and Proulx 2004), the rate of the evolution of life-history traits r_P and r_H are not always exactly equal to the fitness of P and H (see sec. SM6 of the supplemental PDF). The stationary states in the model are evolutionarily singular strategies (α^*, ϵ^*).

Literature Cited

Abdala-Roberts, L., A. Puentes, D. L. Finke, R. J. Marquis, M. Montserrat, E. H. Poelman, S. Rasmann, et al. 2019. Tri-trophic interactions: bridging species, communities and ecosystems. Ecology Letters 22:2151–2167.

Abo-Foul, S., V. I. Raskin, A. Sztejnberg, and J. B. Marder. 1996. Disruption of chlorophyll organization and function in powdery mildew-diseased cucumber leaves and its control by the hyperparasite *Ampelomyces quisqualis*. Phytopathology 86:195–199.

Abrams, P. A., Y. Harada, and H. Matsuda. 1993*a*. On the relationship between quantitative genetic and ESS models. Evolution 47:982–985.

Abrams, P. A., H. Matsuda, and Y. Harada. 1993*b*. Evolutionarily unstable fitness maxima and stable fitness minima of continuous traits. Evolutionary Ecology 7:465–487.

Alizon, S., J. C. de Roode, and Y. Michalakis. 2013. Multiple infections and the evolution of virulence. Ecology Letters 16:556–567.

Alizon, S., A. Hurford, N. Mideo, and M. van Baalen. 2009. Virulence evolution and the trade-off hypothesis: history, current state of affairs and the future. Journal of Evolutionary Biology 22:245–259.

Alizon, S., and M. van Baalen. 2008. Multiple infections, immune dynamics, and the evolution of virulence. American Naturalist 172:E150–E168.

Anagnostakis, S. L. 1982. Biological control of chestnut blight. Science 215:466–471.

Andersen, S. B., M. Ferrari, H. C. Evans, S. L. Elliot, J. J. Boomsma, and D. P. Hughes. 2012. Disease dynamics in a specialized parasite of ant societies. PLoS ONE 7:e36352.

Anderson, R. M., and R. M. May. 1982. Coevolution of hosts and parasites. Parasitology 85:411–426.

Beddington, J., and P. Hammond. 1977. On the dynamics of host-parasite-hyperparasite interactions. Journal of Animal Ecology 46:811–821.

Best, A. 2018. Host-pathogen coevolution in the presence of predators: fluctuating selection and ecological feedbacks. Proceedings of the Royal Society B 285:20180928.

Boldin, B., and O. Diekmann. 2008. Superinfections can induce evolutionarily stable coexistence of pathogens. Journal of Mathematical Biology 56:635–672.

Brännström, Å., J. Johansson, and N. Von Festenberg. 2013. The hitchhiker's guide to adaptive dynamics. Games 4:304–328.

Broom, M., and J. Rychtár. 2013. Game-theoretical models in biology. CRC, Boca Raton, FL.

Brüssow, H., C. Canchaya, and W.-D. Hardt. 2004. Phages and the evolution of bacterial pathogens: from genomic rearrangements to lysogenic conversion. Microbiology and Molecular Biology Reviews 68:560–602.

Carbone, I., Y.-C. Liu, B. I. Hillman, and M. G. Milgroom. 2004. Recombination and migration of *Cryphonectria hypovirus 1* as inferred from gene genealogies and the coalescent. Genetics 166:1611–1629.

Christiansen, F. B. 1991. On conditions for evolutionary stability for a continuously varying character. American Naturalist 138:37–50.

Day, T., and S. R. Proulx. 2004. A general theory for the evolutionary dynamics of virulence. American Naturalist 163:E40–E63.

de Roode, J. C., A. J. Yates, and S. Altizer. 2008. Virulence-transmission trade-offs and population divergence in virulence in a naturally occurring butterfly parasite. Proceedings of the National Academy of Sciences of the USA 105:7489–7494.

Dieckmann, U., and M. Doebeli. 1999. On the origin of species by sympatric speciation. Nature 400:354–357.

Dieckmann, U., J. A. Metz, and M. W. Sabelis. 2005. Adaptive dynamics of infectious diseases: in pursuit of virulence management. Vol. 2. Cambridge University Press, Cambridge.

Doebeli, M. 2011. Adaptive diversification. Monographs in Population Biology. Vol. 48. Princeton University Press, Princeton, NJ.

Doumayrou, J., A. Avellan, R. Froissart, and Y. Michalakis. 2013. An experimental test of the transmission-virulence trade-off hypothesis in a plant virus. Evolution 67:477–486.

Ebert, D., and J. J. Bull. 2003. Challenging the trade-off model for the evolution of virulence: is virulence management feasible? Trends in Microbiology 11:15–20.

Eshel, I. 1983. Evolutionary and continuous stability. Journal of Theoretical Biology 103:99–111.

Faruque, S. M., M. J. Islam, Q. S. Ahmad, A. Faruque, D. A. Sack, G. B. Nair, and J. J. Mekalanos. 2005. Self-limiting nature of seasonal cholera epidemics: role of host-mediated amplification of phage. Proceedings of the National Academy of Sciences of the USA 102:6119–6124.

Fiegna, F., and G. J. Velicer. 2003. Competitive fates of bacterial social parasites: persistence and self-induced extinction of *Myxococcus xanthus* cheaters. Proceedings of the Royal Society B 270:1527–1534.

Geritz, S. A. H., É. Kisdi, G. Meszéna, and J. A. J. Metz. 1998. Evolutionarily singular strategies and the adaptive growth and branching of the evolutionary tree. Evolutionary Ecology 12:35–57.

Geritz, S. A. H., J. A. J. Metz, É. Kisdi, and G. Meszéna. 1997. Dynamics of adaptation and evolutionary branching. Physical Review Letters 78:2024.

Gerlach, D., Y. Guo, C. De Castro, S.-H. Kim, K. Schlatterer, F.-F. Xu, C. Pereira, et al. 2018. Methicillin-resistant *Staphylococcus aureus* alters cell wall glycosylation to evade immunity. Nature 563:705–709.

Ghabrial, S. A., and N. Suzuki. 2009. Viruses of plant pathogenic fungi. Annual Review of Phytopathology 47:353–384.

Hassell, M. 2000. The spatial and temporal dynamics of host-parasitoid interactions. Oxford University Press, Oxford.

Heiniger, U., and D. Rigling. 1994. Biological control of chestnut blight in Europe. Annual Review of Phytopathology 32:581–599.

Holt, R. D., and M. E. Hochberg. 1998. The coexistence of competing parasites. Part II—hyperparasitism and food chain dynamics. Journal of Theoretical Biology 193:485–495.

Kisdi, É. 2006. Trade-off geometries and the adaptive dynamics of two co-evolving species. Evolutionary Ecology Research 8:959–973.

Kisdi, É., S. A. Geritz, and B. Boldin. 2013. Evolution of pathogen virulence under selective predation: a construction method to find eco-evolutionary cycles. Journal of Theoretical Biology 339:140–150.

Kisdi, É., and G. Meszéna. 1993. Density dependent life history evolution in fluctuating environments. Pages 26–62 *in* Adaptation in stochastic environments. Springer, Berlin.

Kiss, L., J. Russell, O. Szentiványi, X. Xu, and P. Jeffries. 2004. Biology and biocontrol potential of *Ampelomyces* mycoparasites, natural antagonists of powdery mildew fungi. Biocontrol Science and Technology 14:635–651.

Lion, S. 2018. Theoretical approaches in evolutionary ecology: environmental feedback as a unifying perspective. American Naturalist 191:21–44.

Lipsitch, M., and E. R. Moxon. 1997. Virulence and transmissibility of pathogens: what is the relationship? Trends in Microbiology 5:31–37.

Liu, Y.-C., R. Durrett, and M. G. Milgroom. 2000. A spatially-structured stochastic model to simulate heterogeneous transmission of viruses in fungal populations. Ecological Modelling 127:291–308.

Matessi, C., and C. Di Pasquale. 1996. Long-term evolution of multilocus traits. Journal of Mathematical Biology 34:613–653.

Matsuda, H., and P. A. Abrams. 1994. Timid consumers: self-extinction due to adaptive change in foraging and anti-predator effort. Theoretical Population Biology 45:76–91.

May, R. M., and M. P. Hassell. 1981. The dynamics of multiparasitoid-host interactions. American Naturalist 117:234–261.

McCallum, H., N. Barlow, and J. Hone. 2001. How should pathogen transmission be modelled? Trends in Ecology and Evolution 16:295–300.

Milgroom, M. G., and P. Cortesi. 2004. Biological control of chestnut blight with hypovirulence: a critical analysis. Annual Review of Phytopathology 42:311–338.

Monod, J. 1949. The growth of bacterial cultures. Annual Review of Microbiology 3:371–394.

Morozov, A., and A. Best. 2012. Predation on infected host promotes evolutionary branching of virulence and pathogens' biodiversity. Journal of Theoretical Biology 307:29–36.

Morozov, A. Y., and M. Adamson. 2011. Evolution of virulence driven by predator-prey interaction: possible consequences for population dynamics. Journal of Theoretical Biology 276:181–191.

Morozov, A. Y., C. Robin, and A. Franc. 2007. A simple model for the dynamics of a host-parasite-hyperparasite interaction. Journal of Theoretical Biology 249:246–253.

Muir, W. M., and R. D. Howard. 1999. Possible ecological risks of transgenic organism release when transgenes affect mating

success: sexual selection and the Trojan gene hypothesis. Proceedings of the National Academy of Sciences of the USA 96:13853–13856.

Nobrega, F. L., A. R. Costa, L. D. Kluskens, and J. Azeredo. 2015. Revisiting phage therapy: new applications for old resources. Trends in Microbiology 23:185–191.

Parratt, S. R., B. Barrès, R. M. Penczykowski, and A.-L. Laine. 2017. Local adaptation at higher trophic levels: contrasting hyperparasite-pathogen infection dynamics in the field and laboratory. Molecular Ecology 26:1964–1979.

Parratt, S. R., and A.-L. Laine. 2016. The role of hyperparasitism in microbial pathogen ecology and evolution. ISME Journal 10:1815–1822.

Parvinen, K. 2005. Evolutionary suicide. Acta Biotheoretica 53:241–264.

Ponciano, J. M., and M. A. Capistrán. 2011. First principles modeling of nonlinear incidence rates in seasonal epidemics. PLoS Computational Biology 7:e1001079.

Svennungsen, T. O., and É. Kisdi. 2009. Evolutionary branching of virulence in a single-infection model. Journal of Theoretical Biology 257:408–418.

Swinton, J., and C. Gilligan. 1999. Selecting hyperparasites for biocontrol of Dutch elm disease. Proceedings of the Royal Society B 266:437–445.

Taylor, D. R. 2002. Ecology and evolution of chestnut blight fungus. Pages 286–296 *in* U. Dieckmann, J. Metz, M. W. Sabelis, and K. Sigmund, eds. Adaptive dynamics of infectious diseases. Cambridge University Press, Cambridge.

Taylor, D. R., A. M. Jarosz, D. W. Fulbright, and R. E. Lenski. 1998. The acquisition of hypovirulence in host-pathogen systems with three trophic levels. American Naturalist 151:343–355.

Taylor, P. D. 1989. Evolutionary stability in one-parameter models under weak selection. Theoretical Population Biology 36:125–143.

Travisano, M. 1997. The effects of toxic metabolites on dynamics and fitness in laboratory populations. Pages 97–112 *in* F. Horikoshi and Kudo, eds. Microbial diversity and biodegradation. Japan Scientific Societies Press, Tokyo.

Webb, C. 2003. A complete classification of Darwinian extinction in ecological interactions. American Naturalist 161:181–205.

Associate Editor: Michael H. Cortez
Editor: Russell Bonduriansky

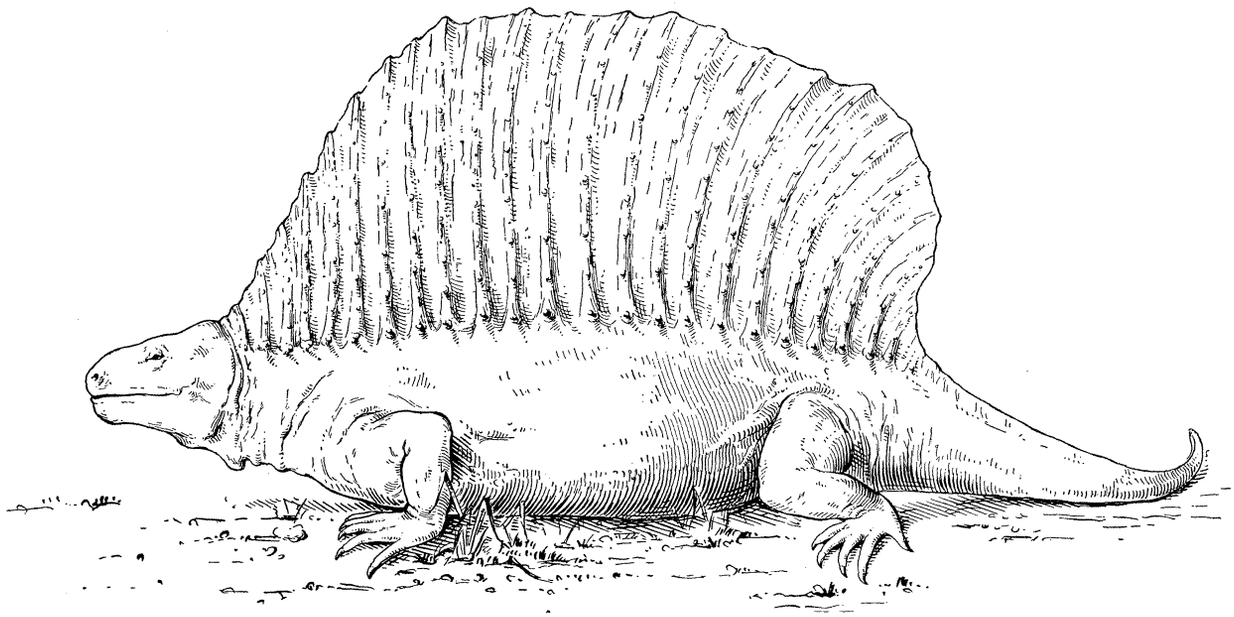

"The author is not in accord with the suggestion made by Jaekel and Abel that the spines were separate, and can see no reason for the suggestion made by the former that the spines were movable. . . . The union of the spines into a thin dorsal fin is far more probable and the idea is supported by the presence of rugosities and the channels of small nutrient vessels such as would lie beneath a thick dermal covering." From "Restoration of *Edaphosaurus cruciger* Cope" by E. C. Case (*The American Naturalist*, 1914, 48:117–121).